



International Agreement Report

Time Step and Mesh Size Dependencies in the Heat Conduction Solution of a Semi-Implicit, Finite Difference Scheme for Transient Two-Phase Flow

Prepared by
R. O'Mahoney

Winfrith Technology Centre
United Kingdom Atomic Energy Authority
Dorchester, Dorset, DT2 8DH
United Kingdom

Office of Nuclear Regulatory Research
U.S. Nuclear Regulatory Commission
Washington, DC 20555

April 1992

Prepared as part of
The Agreement on Research Participation and Technical Exchange
under the International Thermal-Hydraulic Code Assessment
and Application Program (ICAP)

Published by
U.S. Nuclear Regulatory Commission

9206050101 920430
PDR NUREG
IA-0073 R PDR

NOTICE

This report was prepared under an international cooperative agreement for the exchange of technical information.* Neither the United States Government nor any agency thereof, or any of their employees, makes any warranty, expressed or implied, or assumes any legal liability or responsibility for any third party's use, or the results of such use, of any information, apparatus product or process disclosed in this report, or represents that its use by such third party would not infringe privately owned rights.

Available from:

Superintendent of Documents
U.S. Government Printing Office
P.O. Box 37082
Washington, D.C. 20013-7082

and

National Technical Information Service
Springfield, VA 22161

NUREG/IA-0073
AEEW-M2590



International Agreement Report

Time Step and Mesh Size Dependencies in the Heat Conduction Solution of a Semi-Implicit, Finite Difference Scheme for Transient Two-Phase Flow

Prepared by
R. O'Mahoney

Winfrith Technology Centre
United Kingdom Atomic Energy Authority
Dorchester, Dorset, DT2 8DH
United Kingdom

Office of Nuclear Regulatory Research
U.S. Nuclear Regulatory Commission
Washington, DC 20555

April 1992

Prepared as part of
The Agreement on Research Participation and Technical Exchange
under the International Thermal-Hydraulic Code Assessment
and Application Program (ICAP)

Published by
U.S. Nuclear Regulatory Commission

NOTICE

This report is based on work performed under the sponsorship of the United Kingdom Atomic Energy Authority. The information in this report has been provided to the USNRC under the terms of the International Code Assessment and Application Program (ICAP) between the United States and the United Kingdom (Administrative Agreement - WH 36047 between the United States Nuclear Regulatory Commission and the United Kingdom Atomic Energy Authority Relating to Collaboration in the Field of Modelling of Loss of Coolant Accidents, February 1985). The United Kingdom has consented to the publication of this report as a USNRC document in order to allow the widest possible circulation among the reactor safety community. Neither the United States Government nor the United Kingdom or any agency thereof, or any of their employees, makes any warranty, expressed or implied, or assumes any legal liability of responsibility for any third party's use, or the results of such use, or any information, apparatus, product or process disclosed in this report, or represents that its use by such third party would not infringe privately owned rights.

TIME STEP AND MESH SIZE DEPENDENCIES IN THE HEAT CONDUCTION
SOLUTION OF A SEMI-IMPLICIT, FINITE DIFFERENCE SCHEME FOR
TRANSIENT TWO-PHASE FLOW

R O'Mahoney

Summary

This report examines, and establishes the causes of, previously identified time step and mesh size dependencies. These dependencies were observed in the solution of a coupled system of heat conduction and fluid flow equations as used in the TRAC-PF1/MOD1 computer code.

The TRAC-PF1/MOD1 computer code employs a semi-implicit, finite difference solution scheme to solve the differential equations describing heat transfer and two-phase fluid flow; it is commonly used to analyse loss-of-coolant accidents in Pressurised Water Reactors.

The report shows that a significant time step size dependency can arise in calculations of the quenching of a previously unwetted surface. The cause of this dependency is shown to be the explicit evaluation, and subsequent smoothing, of the term which couples the heat transfer and fluid flow equations. An axial mesh size dependency is also identified, but this is very much smaller than the time step size dependency.

The report concludes that the time step size dependency represents a potential limitation on the use of large time step sizes for the types of calculation discussed. This limitation affects the present TRAC-PF1/MOD1 computer code and may similarly affect other semi-implicit finite difference codes that employ similar techniques. It is likely to be of greatest significance in codes where multi-step techniques are used to allow the use of large time steps.

Safety and Engineering Science Division
Winfrith Technology Centre

July 1989

CONTENTS

	<u>PAGE</u>
SECTION 1 INTRODUCTION	1
2 DESCRIPTION OF TRAC-PF1/MOD1	1
3 TRAC-PF1/MOD1 QUENCHING RESULTS	2
4 DETAILED EXAMINATION OF CONDUCTION TERMS	4
4.1 Finite Difference Equation	4
4.2 Surface-to Fluid Effects	4
4.2.1 Explicit Evaluation and Smoothing Effects	5
4.2.2 Time Step Size Effects	6
4.3 Axial Conduction Effects	6
4.4 Quench Front Profiles	7
4.4.1 Calculation with 0.25 mm Minimum Axial Mesh	7
4.4.2 Calculation with 0.25 mm Mesh and 0.3 ms Time Step	8
4.4.3 <u>AXIAL</u> Term Time Step Dependency	8
4.4.4 Calculations with no Axial Conduction	9
4.4.5 Axial Mesh Size Effects	10
5 SUMMARY AND CONCLUSIONS	10
6 REFERENCES	12

FIGURES

PAGE

1	Rod surface temperatures at 5 elevations, for 4 different mesh sizes. Min axial meshes are: CONT=2.5 mm, SHORT=0.25 mm, LONG=0.1 mm, THICK=0.05 mm.	13
2	Axial profile of rod surface temperature at 4 different times. Profiles at 0, 10, 20 and 30 seconds, for 0.1 mm axial mesh.	14
3	Rod surface temperatures at 5 elevations, for 3 calculations. Calculations are: CONT=0.25 mm, SHORT=0.05 mm, LONG=0.25 mm + 0.3 ms step.	15
4	Surface-to-fluid heat transfer coefficient vs temperature, at 20 seconds. TRAC calculation with 0.25 mm min mesh + theoretical heat transfer.	16
5	Surface-to-fluid heat flux vs temperature, at 20 seconds. TRAC calculation with 0.25 mm min mesh + theoretical heat flux.	17
6	Surface-to-fluid heat transfer coefficient vs temperature, at 20 seconds. TRAC calculation with 0.25 mm min mesh, no smoothing + theoretical heat transfer.	18
7	Surface-to-fluid heat transfer coefficient vs temperature, at 20 seconds. TRAC calculation with 0.25 mm min mesh, 0.3 ms time step + theoretical heat transfer.	19
8	Surface-to-fluid heat flux vs temperature, at 20 seconds. TRAC calculation with 0.25 mm min mesh, 0.3 ms time step + theoretical heat transfer.	20
9	Rod surface temperatures at 7 elevations, for 3 no-axial calculations. Calculations are: CONT=0.25 mm, SHORT=0.25 mm + 0.3 ms, LONG=0.05 mm + 0.3 ms.	21
10	Surface-to-fluid heat flux vs temperature, at 20 seconds. TRAC calculation, no axial conduction, 0.25 mm minimum mesh + theoretical heat flux.	22
11	Surface-to-fluid heat flux vs temperature, at 20 seconds. TRAC calculation, no axial conduction, 0.25 mm min mesh, 0.3 ms time step + theoretical heat flux.	23
12	Heat conduction equation: quench front profile at 20 seconds. TRAC calculation with 0.25 mm min mesh.	24
13	Heat conduction equation: quench front profile at 20 seconds. TRAC calculation with 0.25 mm min mesh (exploded view).	25

FIGURES (Continued)

	<u>PAGE</u>
14 Heat conduction equation: quench front profile at 20 seconds. TRAC calculation with 0.25 mm min mesh, 0.3 ms time step.	26
15 Heat conduction equation: quench front profile at 20 seconds. TRAC calculation with 0.25 mm min mesh, 0.3 ms time step (exploded view).	27
16 Surface-to-fluid heat flux vs temperature, at 20 seconds. TRAC calculation with 0.25 mm min mesh, 0.3 ms step, reduced CHF + theoretical heat flux.	28
17 Heat conduction equation: quench front profile at 20 seconds. TRAC calculation with 0.25 mm min mesh, 0.3 ms step, reduced heat flux.	29
18 Heat conduction equation: quench front profile at 20 seconds. TRAC calculation with no axial conduction, 0.25 mm min mesh.	30
19 Heat conduction equation: quench front profile at 20 seconds. TRAC calculation with no axial conduction, 0.25 mm min mesh (exploded view).	31
20 Heat conduction equation: quench front profile at 20 seconds. TRAC calculation with no axial conduction, 0.25 mm min mesh, 0.3 ms, time step.	32
21 Heat conduction equation: quench front profile at 20 seconds. TRAC with no axial conduction, 0.25 mm min mesh, 0.3 ms step (exploded view).	33
22 Surface-to-fluid heat flux vs temperature, at 20 seconds. TRAC calculation with 0.1 mm min mesh, 0.3 ms time step + theoretical heat transfer.	34
23 Heat conduction equation: quench front profile at 20 seconds. TRAC calculation with 0.1 mm min mesh, 0.3 ms time step.	35
24 Heat conduction equation: quench front profile at 20 seconds. TRAC calculation with 0.1 mm min mesh, 0.3 ms time step (exploded view).	36
25 Rod surface temperatures at 5 elevations, for 3 calculations. Calculations are: CONT=0.25 mm, SHORT=0.25 mm + 0.3 ms, LONG=0.1 mm + 0.3 ms.	37

NOMENCLATURE

A	Surface area
C _p	Specific heat at constant pressure
h	Heat transfer coefficient
K	Thermal conductivity
q'''	Volumetric heat generation rate
Q	Heat transfer (energy)
r	Radial cylindrical coordinate
ρ	Density
T	Temperature
t	Time
z	Axial cylindrical coordinate

(SI units)

1 INTRODUCTION

A previous study, [1], examined certain axial effects in the heat conduction solution of the transient, two-phase flow computer code TRAC-PF1/MOD1 [2]. Calculations which simulated the quenching of the surface of a nuclear fuel rod were seen to have time step size and, to a lesser extent, axial mesh size dependencies. The purpose of the present paper is to examine and explain these dependencies. Similar dependencies may well arise in other computer codes which employ semi-implicit, finite difference solution schemes.

Section 2 of this paper gives a brief description of the TRAC-PF1/MOD1 computer code. This section concentrates on the particular aspects of the code that are relevant to this study.

Section 3 presents some results from the TRAC-PF1/MOD1 calculations which demonstrate the time step size and axial mesh size dependencies.

In Section 4 a more detailed examination is made of the individual terms that contribute to the heat conduction equation. Various graphical surfaces are generated by over-plotting the results from several successive time steps.

Finally, Section 5 presents the overall conclusions of this study.

2 DESCRIPTION OF TRAC-PF1/MOD1

TRAC-PF1/MOD1 is used to perform analyses of Loss-of-Coolant accidents and other transients in Pressurised Water Reactors (PWR's). It is also used to analyse a wide range of related thermal-hydraulic experiments.

The basic operation of the code is to solve the time-dependent partial differential equations describing two-phase flow (water and steam) and heat transfer, by finite difference methods. The heat transfer equations are treated by using a semi-implicit differencing technique. The fluid dynamics equations are solved for one-dimensional components, such as pipes, using a multistep procedure that allows the material Courant condition to be violated. For a three-dimensional component, such as the reactor vessel, a semi-implicit differencing scheme is used. The combined finite-difference equations form a system of coupled, non-linear equations. They are solved by a Newton iteration procedure for each time step.

One aspect of the numerical scheme that is relevant to the subsequent discussion in this paper relates to the coupling between the heat transfer equations and the hydrodynamic equations. The heat transfer equations might, for example, be used to model the two-dimensional heat conduction within a heated cylindrical rod. The coupling with the hydrodynamics equations

takes place via the surface heat transfer between the rod and the surrounding fluid. This surface heat transfer will be dependent on the rod surface temperature and several of the fluid's properties; it provides a surface boundary condition for the heat conduction equation and contributes to the energy and mass conservation equations for the fluid. The surface boundary condition for the heat conduction equation, at time step (n+1), is of the form:-

$$K \frac{\partial T}{\partial r} = - h^n (T_{\text{surface}}^{n+1} - T_{\text{fluid}}^{n+1}) \quad (1)$$

The surface to fluid heat transfer contribution to the energy equation, for time step (n+1), is of the form:-

$$Q_{\text{surface to fluid}} = h^n A (T_{\text{surface}}^n - T_{\text{fluid}}^{n+1}) \Delta t \quad (2)$$

The point of particular significance in this heat transfer coupling is that the surface heat transfer coefficient is evaluated explicitly; it is calculated using rod and fluid conditions from the previous time step. In later sections of this paper it is shown that this explicit evaluation, taken together with the smoothing that is applied to the heat transfer coefficient, can significantly affect the calculated surface heat transfer.

3 TRAC-PF1/MOD1 QUENCHING RESULTS

The calculations originally reported in [1] were hypothetical simulations of a 1 m, vertical, length of nuclear fuel rod inside a cylindrical pipe. The calculations were initialised with the rod temperatures sufficiently high that the surface, for elevations above the very bottom, could not be wetted. A constant flow of water was introduced at the bottom of the pipe; the resulting cooling and ultimate quenching of the rod surface by the fluid, was then calculated.

Some typical results from the TRAC-PF1/MOD1 calculation are presented in Figure 1. This Figure shows rod surface temperatures, at five elevations, plotted against time, for four separate calculations. The differences between the four calculations lie in the size of the smallest axial mesh used in the finite difference representation of the fuel rod. This mesh is separate from the mesh used to solve the fluid flow equations, which was unchanged. It can be seen from Figure 1 that there is a wide variation in the times at which the rod surface temperature, for any particular elevation, quenches (ie falls rapidly to the fluid saturation temperature). It is not immediately apparent why changing the axial mesh size should have this effect.

The reason for wanting to change the axial mesh can best be explained by reference to Figure 2. This Figure shows axial profiles of the rod surface temperature at successive times, for one of the calculations represented in Figure 1. It can be seen from Figure 2 that shortly after the start of the calculated transient a sharp, or steep, temperature gradient develops; this gradient, or quench front, effectively separates the hot unquenched region from the cooler quenched region. As the transient continues this quench front progress along the rod. The reason for changing the axial mesh size in the original TRAC-PF1/MOD1 calculation was to identify and examine the effects it might have on the quench front progression.

The quench front region itself is typically only a few millimetres wide. The TRAC-PF1/MOD1 solution scheme attempts to resolve this very steep temperature gradient by inserting an extra row of heat conduction mesh points, wherever the temperature difference between adjacent surface nodes exceeds a user-input value. This value is typically 3°K for mesh points in the vicinity of the quench front. In order to prevent an excessively large number of mesh points being used the user also specifies a lower bound on the axial mesh spacing that can have an extra row of mesh points inserted. The four calculations represented in Figure 1 used differing values of this lower bound; the effective minimum mesh sizes were 2.5 mm, 0.25 mm, 0.1 mm and 0.05 mm. Figure 1 shows that reducing the lower bound causes the quench front to progress more quickly; it also causes the quenching to occur at slightly higher surface temperatures.

The semi-implicit nature of the heat conduction solution in TRAC-PF1/MOD1 leads to additional complications in trying to understand the apparent mesh size dependency.

TRAC-PF1/MOD1 uses a two-dimensional (r,z) cylindrical heat conduction equation. Azimuthal symmetry is assumed. The differential equation can be written as

$$\rho c_p \frac{\partial T}{\partial t} = \dot{q}'' + \frac{1}{r} \frac{\partial}{\partial r} (rk \frac{\partial T}{\partial r}) + \frac{\partial}{\partial z} (k \frac{\partial T}{\partial z}) \quad (3)$$

The finite difference form of equation (3), implemented in TRAC-PF1/MOD1, has implicit differencing in the radial (r) direction and explicit differencing in the axial (z) direction. The explicit differencing used for the axial term in Equation (3) leads to a stability restriction on the maximum time step size (Δt_{max}) for a particular minimum axial mesh size (Δz_{min}). This restriction is of the form -

$$\Delta t_{max} = \Delta z_{min}^2$$

Thus, for the four calculations represented in Figure 1, changing the lower bound on the mesh size has also changed the time step size in the calculations. The effect of reducing the time step alone can be judged from Figure 3. This Figure shows results from three calculations; a large mesh size case, a small mesh size case, and a case with a large mesh size but a time step restricted to 0.3 milliseconds. (0.3 milliseconds was the average time step size of the small mesh size calculation). Figure 3 shows that most of the effect seen in reducing the mesh size is in fact due to the resultant reduction in time step. This time step size, and to a lesser extent mesh size, dependency is further examined and explained in Section 4.

4 DETAILED EXAMINATION OF CONDUCTION TERMS

The previous section highlighted the fact that reducing the time step size used in the quenching calculations had changed the results. In particular, it had caused the rod surface to quench at a faster rate and from a higher temperature. To a lesser extent, reducing the axial mesh size had a similar effect. This behaviour is now examined in more detail by considering the individual terms of the heat conduction solution.

4.1 Finite Difference Equation

TRAC-PF1/MOD1 solves a finite difference form of equation (3); this is obtained by applying an integral method to an appropriate differential volume. If the resulting finite difference equation for each node is divided by ρC_p and by the node volume, then an equation of the form:

$$\text{TOTAL} = \text{GENERATION} + \text{RADIAL} + \text{AXIAL} \quad (3a)$$

(where each term is in °K/sec)

can be written for each node in turn. The heat generation occurs internally within the rod so that for the surface nodes the GENERATION term in Equation (3a) will be zero. For the nodes of interest in this section, i.e. close to the quench front, the automatic mesh refinement will cause all the node sizes to be close to the minimum allowed.

4.2 Surface-to-Fluid Effects

Plots presented later in this section show the individual terms of Equation (3a), for the surface nodes, drawn as a function of the wall temperature. First, however, it is useful to examine one component of the RADIAL term, namely the surface heat transfer between the rod and the coolant.

Figure 4 shows a plot of surface heat transfer coefficient versus surface temperature. Results from the TRAC-PF1/MOD1 calculation with a 0.25 mm minimum axial mesh are displayed as a sequence of points, drawn as numbers. The results are taken from each surface node for 11 consecutive time steps at approximately 20 seconds into the calculation. The fluid conditions will

normally only change slightly during 11 time steps so it is reasonable to expect that the points representing heat transfer coefficient versus wall temperature will lie on a curve. In Figure 4 the points labelled "1" are from time step 1 of the sequence and so on. Points labelled "*" and "A" are for time steps 10 and 11 respectively. The curve traced out by the points labelled "1" to "A" is the effective heat transfer curve for this particular calculation, at 20 seconds. Figure 4 also shows the theoretical heat transfer curve derived for the particular fluid conditions present in the TRAC-PF1/MOD1 calculation. This curve was calculated by evaluating the TRAC-PF1/MOD1 heat transfer correlation separately, in a stand-alone manner, for the range of surface temperatures of interest.

Figure 4 shows that once a surface node is cooled below approximately 600°K its surface heat transfer coefficient increases sharply. A theoretical maximum is shown to be reached at approximately 470°K; this corresponds to the point of critical heat flux. However, the most striking feature of Figure 4 is the fact that the achieved, or effective, heat transfer curve is significantly below the theoretical curve. Many values are 40-50% below the theoretical values and the critical heat flux temperature appears to be 20°K lower. These differences are further highlighted in Figure 5 which shows the surface heat flux values corresponding to the coefficients given in Figure 4.

4.2.1 Explicit Evaluation and Smoothing Effects

The differences observed between the effective and theoretical heat transfer curves arise from two separate aspects of the TRAC-PF1/MOD1 solution scheme. Firstly the explicit evaluation of the surface heat transfer coefficients; this means, for example, that the surface temperature from the previous time step is used to evaluate the new coefficient. Secondly, the smoothing and limiting techniques applied to the calculated heat transfer coefficient; 55% under-relaxation is used (55% old-time value + 45% new-time value), followed by the restriction that, essentially, the resulting new value is no more than twice the old-time value. These techniques are applied on a per-time step basis and not on a per-unit time basis; thus, for example, during the rapid increase in coefficient shown in Figure 4 some time step size dependency will occur.

The TRAC-PF1/MOD1 results shown in Figure 6 will allow these two aspects of the solution scheme to be considered separately. The results shown in Figure 6 are from a calculation in which the surface heat transfer smoothing and limiting have been removed. The theoretical heat transfer curve has been derived for the fluid conditions present at the end of the time step sequence. The effect of the explicit evaluation of the surface heat transfer coefficient can be clearly seen in Figure 6 for time steps 3 onwards (ie points numbered 3-9, * and A). For example, the point marked "4", at approximately 485°K, has a heat transfer value that corresponds to the theoretical curve evaluated at the temperature of the point marked "3", close to 500°K. Similarly the point "5" value corresponds to the point "4" temperatures and

so on. (This correspondence does not work in Figure 6 for the points marked "3", "2" and "1" because the fluid conditions at those time steps were slightly different to those used to derive the theoretical curve). In other words the surface temperature T_s is at time step $(n+1)$, but the heat transfer coefficient h_s is at time step (n) . This point is confirmed in the formulation of equation (1).

Figure 6 demonstrates that, in a region where the heat transfer coefficient is changing rapidly, the explicit evaluation of the coefficient can lead to a significant deviation of the effective heat transfer curve from the theoretical one. In Figure 4 the deviation also includes the under-relaxation and limiting effects: the difference between the effective and theoretical heat transfer is greater, particularly with regard to the peak value.

4.2.2 Time Step Size Effects

The calculation for which results were presented in Figure 4 used time steps that were in the range of 5-10 milliseconds. Figure 7 shows results from an equivalent calculation in which the time step was constrained to be no greater than 0.3 milliseconds. The TRAC-PF1/MOD1 calculated values have been drawn every 24 time steps, ie every 7.2 milliseconds, as this corresponds to the average time step size of the earlier calculation. Figure 7 shows that reducing the time step size has caused the effective heat transfer curve to follow closely the theoretical curve. Figure 8 shows the surface heat flux values corresponding to the coefficients given in Figure 7. A comparison with Figure 5 emphasises the effect of reducing the time step size.

Clearly, reducing the time step size has led to an increase in the effective surface heat flux for surface temperatures between approximately 450°K and 620°K. This is likely to be a significant factor in explaining the time step size effect seen in Figure 2, for example. However, as the next subsection shows, the presence of axial effects must also be taken into account.

4.3 Axial Conduction Effects

In an attempt to isolate the separate contributions of the RADIAL and AXIAL terms of equation (3a) several TRAC-PF1/MOD1 calculations were carried out with the AXIAL term artificially set to zero. This prevents any axial conduction of heat within the rod. The results, shown in Figure 9, are somewhat surprising. With the AXIAL term removed the calculations show virtually no sensitivity to either time step or axial mesh size.

Figure 10 shows the surface heat flux, plotted as a function of surface temperature, for the first NO-AXIAL conduction calculation. The TRAC-PF1/MOD1 results are similar to those shown in Figure 5 for the standard calculation; the effective heat flux curve is again significantly below the theoretical curve. Figure 11 shows the equivalent results from the NO-AXIAL conduction calculation with the time step restricted to

0.3 milliseconds. The TRAC-PF1/MOD1 results now closely follow the theoretical curve in a similar manner to the standard calculation results presented in Figure 8.

This shows that reducing the time step size in a calculation without axial conduction causes the effective surface heat flux curve to follow closely the theoretical curve. However, this does not affect the overall quenching behaviour to any significant effect. The time step size effect seen in the standard calculations must, therefore, depend on more than just the change in the effective surface heat transfer.

4.4 Quench Front Profiles

In previous sections effective surface heat transfer curves have been generated by over-plotting heat transfer values from a sequence of consecutive time steps. A similar technique can be used to generate a quench front profile of the individual terms of equation (3a), for nodes at the rod surface.

4.4.1 Calculation With 0.25 mm Minimum Axial Mesh

Figure 12 shows the quench front profile at 20 seconds for the standard TRAC-PF1/MOD1 calculation with a 0.25 mm minimum axial mesh. Points labelled "A" represent the magnitude of the AXIAL term of equation (3a), points labelled "R" represent the RADIAL term and points labelled "T" represent the TOTAL term, ie the sum of the AXIAL and RADIAL term. For the sequence of 11 time steps plotted in Figure 12 the points representing the separate terms trace out an effective quench front profile.

The role of the AXIAL term can be readily seen from Figure 12. At the high temperature end of the region the AXIAL term is negative ie tending to cool the rod surface. For temperatures above 550°K the AXIAL term makes up almost all of the TOTAL term. (The RADIAL term has positive values above approximately 585°K because the heat being transferred from inside the rod to the surface exceeds that being transferred from the surface to the fluid). At the low temperature end of the region the AXIAL term is positive ie it is opposing the cooling rate generated by the larger negative RADIAL term. Thus, the overall effect of the AXIAL term is to transfer heat from the high temperature end to the low temperature end where the RADIAL term, largely governed by the surface-to-fluid heat flux, is large and negative.

In Figure 12 the magnitude of the TOTAL ($\partial T/\partial t$) term becomes small, for temperatures above approximately 655°K. This corresponds to the temperature of the "knee" in the temperature versus time plot for the 2.5 millimetre minimum mesh calculation, shown in Figure 1. For temperatures above this value the rod surface is cooled comparatively slowly. However, for temperatures below this value the rate of temperature fall increases very rapidly, until the surface is quenched. It can be seen from Figure 12 that, at least for this calculation, the

temperature at which this knee occurs is governed by the onset of the large negative AXIAL values.

The movement of the quench front region along the rod can conveniently be characterised by the movement along the rod of the knee in the temperature profile. The actual temperature at which the knee is maintained will be dependent on the details of the heat conduction solution within the quench front region itself. Figure 13 presents an exploded view of the AXIAL and RADIAL terms taken from Figure 12 in the region of the knee. For temperatures above 650°K it can be seen that the AXIAL term is essentially zero and the RADIAL term is negative (ie cooling the surface) and increasing in magnitude with increasing surface temperature. For temperatures below 660°K the RADIAL term becomes negligible and the AXIAL term very rapidly becomes large and negative. This large negative AXIAL term rapidly cools the cladding surface and allows the quench front or temperature knee to move forward.

4.4.2 Calculation With 0.25 mm Minimum Mesh and 0.3 ms Time Step

Figure 14 presents the quench front profile at 20 seconds for the standard calculation with the reduced time step size. Comparison with Figure 12 shows that the magnitude of the peak negative RADIAL term has increased significantly; this is in line with the increased surface heat flux seen by comparing Figure 8 with Figure 5. The magnitudes of the peak AXIAL terms (positive at low temperatures, negative at high temperatures) have also increased significantly, leading to increased magnitude TOTAL term values. In particular, the increased magnitude negative AXIAL terms at high temperatures have moved the temperature of the knee up by approximately 20°K. This is borne out by comparing the temperature versus time profiles shown in Figure 3. An exploded view of the AXIAL and RADIAL terms close to the knee is given in Figure 15. Comparison with Figure 13 shows that the RADIAL terms ahead of the knee, from the two calculations, lie approximately on the same curve.

Figure 14 shows that with the reduced time step the magnitude of the AXIAL (and hence TOTAL) term increases more rapidly, as the surface temperature falls below the knee temperature, than for the standard calculation shown in Figure 12. This is consistent with the observed faster progression of the knee in the small time step calculation.

Thus the observed time step size dependency appears to be related to the increased magnitude AXIAL terms at high temperatures. Two questions remain unresolved however: why are the AXIAL terms increased in magnitude, and why does the calculation with no axial conduction show no time step size dependency. These two questions are now addressed in turn.

4.4.3 AXIAL Term Time Step Dependency

The significant increase in the AXIAL term magnitude shown in Figure 14 could be due to two possible effects. Firstly, the

large increase in the peak RADIAL term magnitude will have changed the axial temperature profile in the quench front region. This is likely to change the AXIAL term values as they are, essentially, derived from the axial temperature profile. Secondly, reducing the time step size may in itself have changed the AXIAL term values as they are evaluated explicitly. To resolve this issue a calculation has been performed using the reduced time step size but with the surface-to-fluid heat flux modified so that it remains at the level shown in Figure 5 rather than the increased level shown in Figure 8. This was achieved by reducing the critical heat flux value (CHF) used by TRAC-PF1/MOD1 in evaluating the heat transfer coefficients.

Figure 16 shows the effective surface heat flux curve from this new reduced-time step calculation. It is in fact quite close to the effective curve presented in Figure 5 for the original calculation. Figure 17 shows the quench front profile for the new calculation at 20 seconds. Both the RADIAL and AXIAL term curves are very similar to the corresponding curves shown in Figure 12 for the original calculation. Thus the AXIAL term values have no time step size dependency of their own (within the time step range considered) but rather they reflect the time step size dependency of the RADIAL term. This in turn reflects the time step size dependency of the surface-to-fluid heat flux; as previously shown this is due to the explicit heat transfer evaluation and smoothing techniques inherent in the solution scheme.

4.4.4 Calculations With No Axial Conduction

Figures 10 and 11 showed the effective surface-to-fluid heat flux curves for two calculations with no axial conduction. Reducing the time step size to 0.3 milliseconds caused the effective curve to follow the theoretical curve (Figure 11) but did not, however, change the overall quenching behaviour (Figure 9).

Figure 18 shows the quench front profile for the large time step calculation. As the AXIAL term is zero the TOTAL term is simply equal to the RADIAL term. The effective RADIAL term curve in Figure 18 is similar to the RADIAL term curve shown in Figure 12 for the standard calculation. However, the lack of an AXIAL term means that the T_{min} term becomes small at a lower temperature than in Figure 12; the temperature knee is maintained at a lower temperature. This is confirmed by the temperature versus time profiles shown in Figure 9. Figure 18 also shows that the magnitude of the TOTAL term increases slightly less rapidly, as the surface temperature falls below the knee temperature, than for the standard calculation. This is consistent with the slower progression of the quench front in the calculation with no axial conduction. Figure 19 shows an exploded view of the TOTAL term in the region of the temperature knee. A comparison with the standard calculation results, given in Figure 13, shows that the RADIAL term values lie essentially on the same effective curve. However, in the no axial conduction calculation the knee is maintained at a lower temperature.

The quench front profile for the no axial conduction calculation with the reduced time step size is presented in Figure 20. The peak magnitude of the RADIAL term has increased, compared to Figure 18, in line with the increase in the surface-to-fluid heat flux shown in Figure 11. However, at the high temperature end of the region the values are unchanged. This is further borne out in the exploded view shown in Figure 21.

Thus in a calculation with no axial conduction, although the peak TOTAL term magnitude is increased, the TOTAL term values at the high temperature end of the quench front region are unchanged when a small time step size is used. This is consistent with the observation that the overall quench front movement is unchanged when a small time step size is used.

4.4.5 Axial Mesh Size Effects

Having established and examined the time step size dependency it is now worthwhile examining any mesh size effects. TRAC-PF1/MOD1 will normally automatically reduce the time step size when small axial mesh sizes are used, because of the explicit evaluation of the axial terms. Therefore, to establish any genuine mesh size effects a comparison has to be made with a calculation that already uses a sufficiently small time step size.

A calculation has been performed using a 0.1 mm minimum axial mesh and a 0.3 millisecond time step size. Figure 22 shows the effective surface-to-fluid heat flux curve for this calculation; this can be compared to the curve in Figure 8, which used a 0.25 mm minimum mesh. The two effective curves are very similar; the smaller mesh curve lies slightly closer to the theoretical curve at the peak value. The smaller mesh size gives more nodes, and hence a better resolution, in the region of peak surface-to-fluid heat transfer values.

Figure 23 shows the quench front profile for the new calculation; this can be compared to Figure 14 for the larger mesh size results. The results are again very similar apart from the peak AXIAL and RADIAL values at the low temperature end of the region. An exploded view of the AXIAL and RADIAL terms at the high temperature end of the region is shown in Figure 24. The results are very similar to those shown in Figure 15 for the larger mesh size calculation. This suggests that the overall quench front progress should be very similar for the two calculations.

The surface temperatures versus time for the new calculation are shown in Figure 25. A comparison is made with the larger mesh size calculation and also the original larger time step size calculation. The new calculation shows that there is a small axial mesh size dependency, but that it is very small compared to the time step size dependency.

5 SUMMARY AND CONCLUSIONS

The purpose of this paper is to examine and explain the time step and mesh size dependencies observed in calculations of the

quenching of a nuclear fuel rod. Both effects have been shown to arise from an underlying dependency in the surface-to-fluid heat transfer. The time step dependency occurs because the heat transfer coefficient is evaluated explicitly, ie using values from the previous time step, and because under-relaxation is applied to the newly calculated coefficient. This dependency will be particularly noticeable whenever the heat transfer coefficient is changing significantly from one time step to the next, such as occurs during quenching. The smaller mesh size dependency appears to arise from changes in the spatial resolution at the calculated heat transfer coefficient close to its peak value.

The paper has shown that changes in the surface-to-fluid heat transfer affect the overall quenching behaviour by virtue of changing the axial temperature profile; this changes the axial conduction terms in the overall rod conduction equation. It is changes in the axial conduction terms, at the high temperature end of the quench front region, that alter the overall quench front progression. In calculations where the axial conduction term was artificially removed, changes to the surface-to-fluid heat transfer did not affect the overall quenching behaviour.

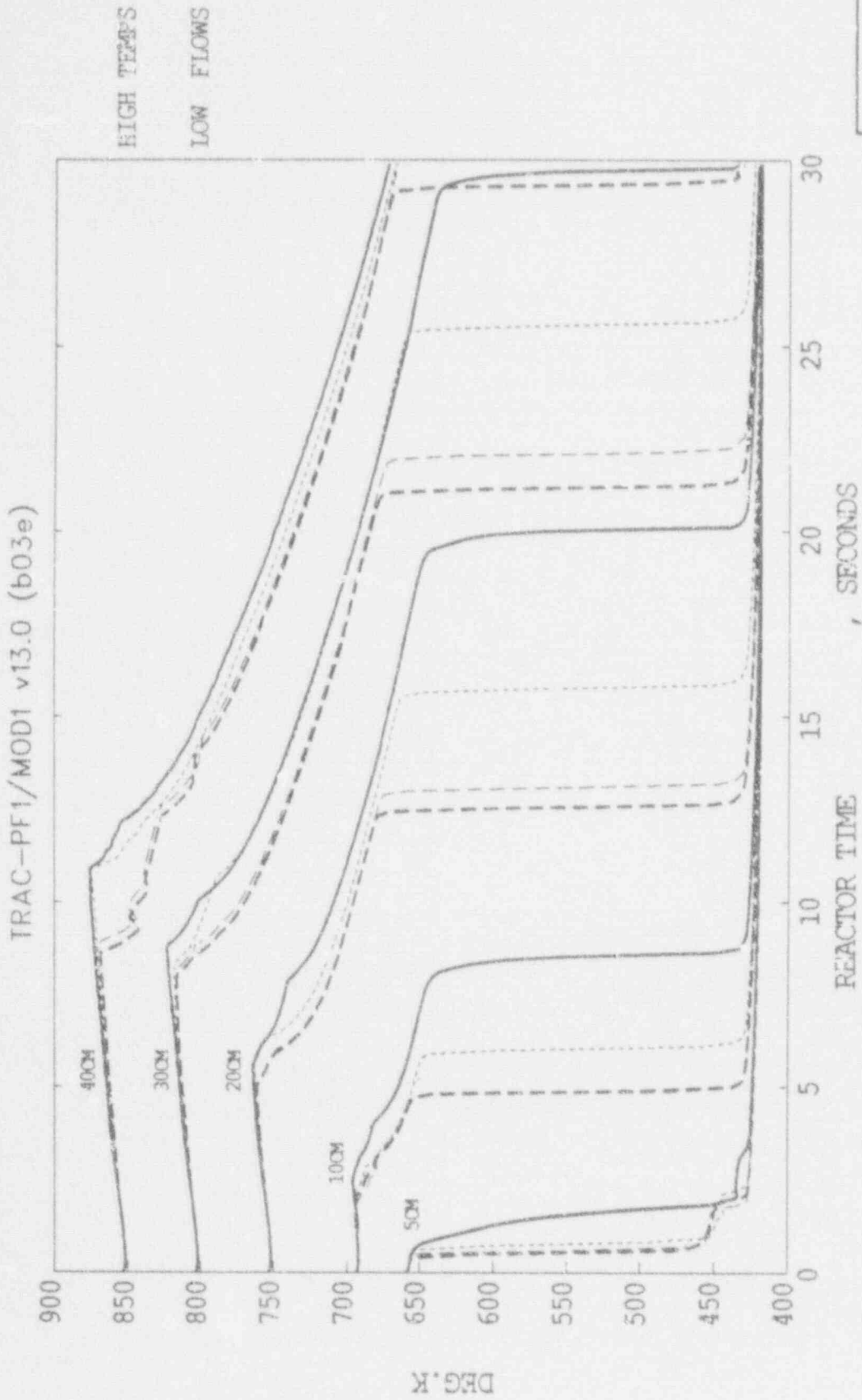
The findings can be summarised in the following conclusions:-

- 5.1 The studies described in this report have identified a significant time step size dependency in the solution obtained from a coupled system of heat transfer and two-phase flow partial differential equations.
- 5.2 The time step size dependency of the solution arises from the time step size dependency of the surface-to-fluid heat flux; this flux is the coupling between the heat transfer equations and the fluid flow equations. The dependency occurs as a result of the explicit evaluation of the surface-to-fluid heat transfer coefficient, and as a result of the time step-to-time step smoothing techniques applied to the coefficient.
- 5.3 For the TRAC-PF1/MOD1 quenching calculations described in the report the time step size dependency of the solution disappears if the axial conduction term of the heat conduction equation is removed. This is because the surface-to-fluid heat flux time step dependency affects the overall solution only by changing the size of the axial conduction terms.
- 5.4 The studies described in this report have also identified a small axial mesh size dependency; this is, however, much smaller than the time step size dependency. This dependency again appears to arise from a small mesh size dependency of the surface-to-fluid heat transfer, mainly in the region of high and rapidly changing heat transfer values.

- 5.5 The time step size dependency represents a potential problem in the use of the TRAC-PF1/MOD1 code, with regard to running times. The numerical solution scheme for one-dimensional components employs a multistep procedure that allows the material Courant condition to be violated. This ability to use large time step sizes will be restricted if small time steps are needed for the heat transfer evaluation part of the scheme. Further work is needed to improve or replace the explicit heat transfer evaluation and to remove the time step size dependency from the heat transfer smoothing techniques.

6 REFERENCES

- (1) O'Mahoney, R. A Study of Axial Effects in the TRAC-PF1/MOD1 Heat Conduction Solution During Quenching. AEEW - M 2552, PWR/HTWG/P(89)686, June 1989.
- (2) TRAC-PF1/MOD1. An Advanced Best-Estimate Computer Program for Pressurised Water Reactor Analysis. Los Alamos National Laboratory Report. LA-10157-MS, NUREG/CR-3858.



Winfrith

FIGURE 1

ROD SURFACE TEMPERATURES AT 5 ELEVATIONS, FOR 4 DIFFERENT MESH SIZES
MIN AXIAL MESHES ARE: CONT=2.5MM, SHORT=0.25MM, LONG=0.1MM, THICK=0.05MM

FIGURE 1

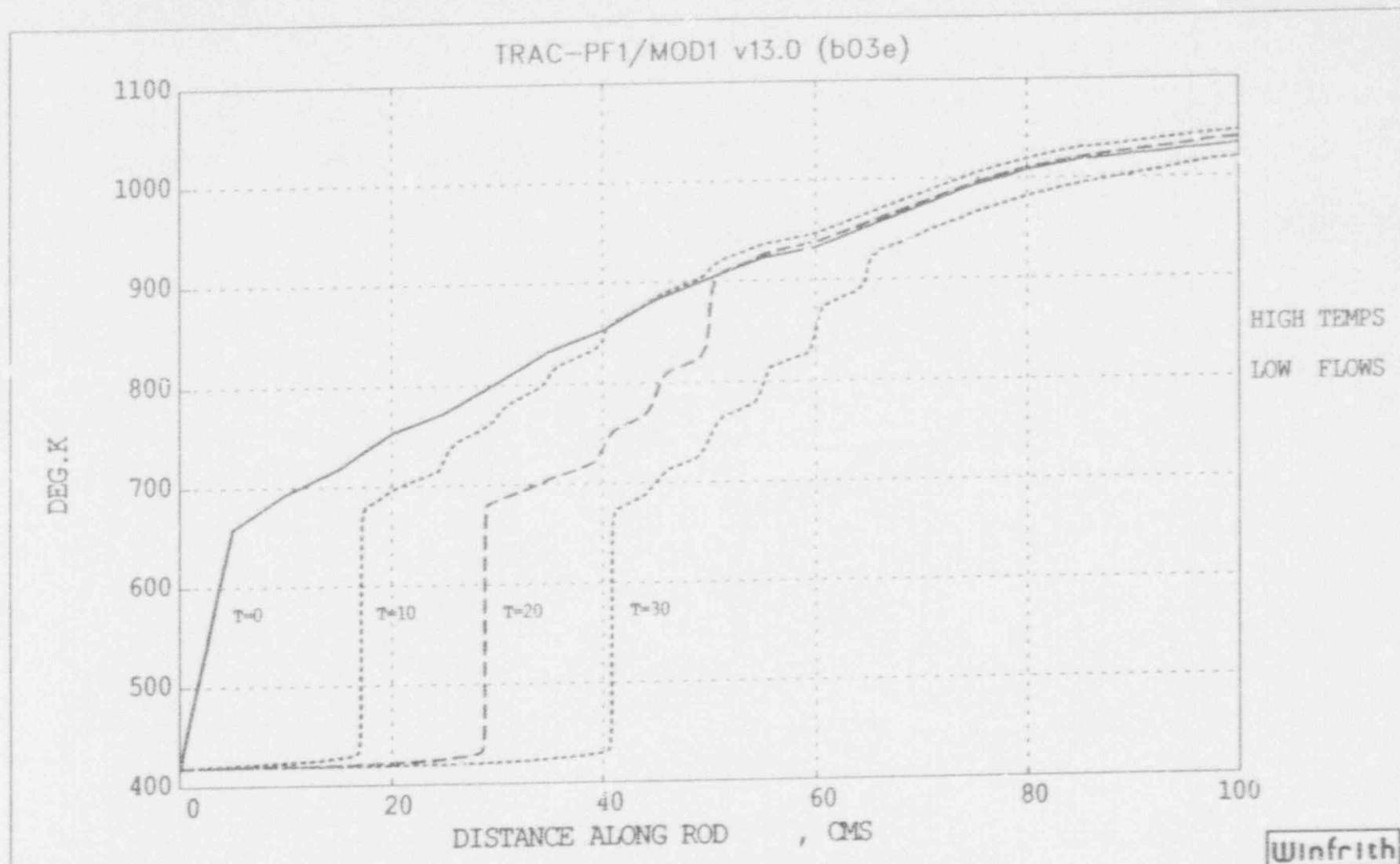


FIGURE 2

AXIAL PROFILE OF ROD SURFACE TEMPERATURE AT 4 DIFFERENT TIMES
PROFILES AT 0, 10, 20 & 30 SECS, FOR 0.1MM MIN AXIAL MESH

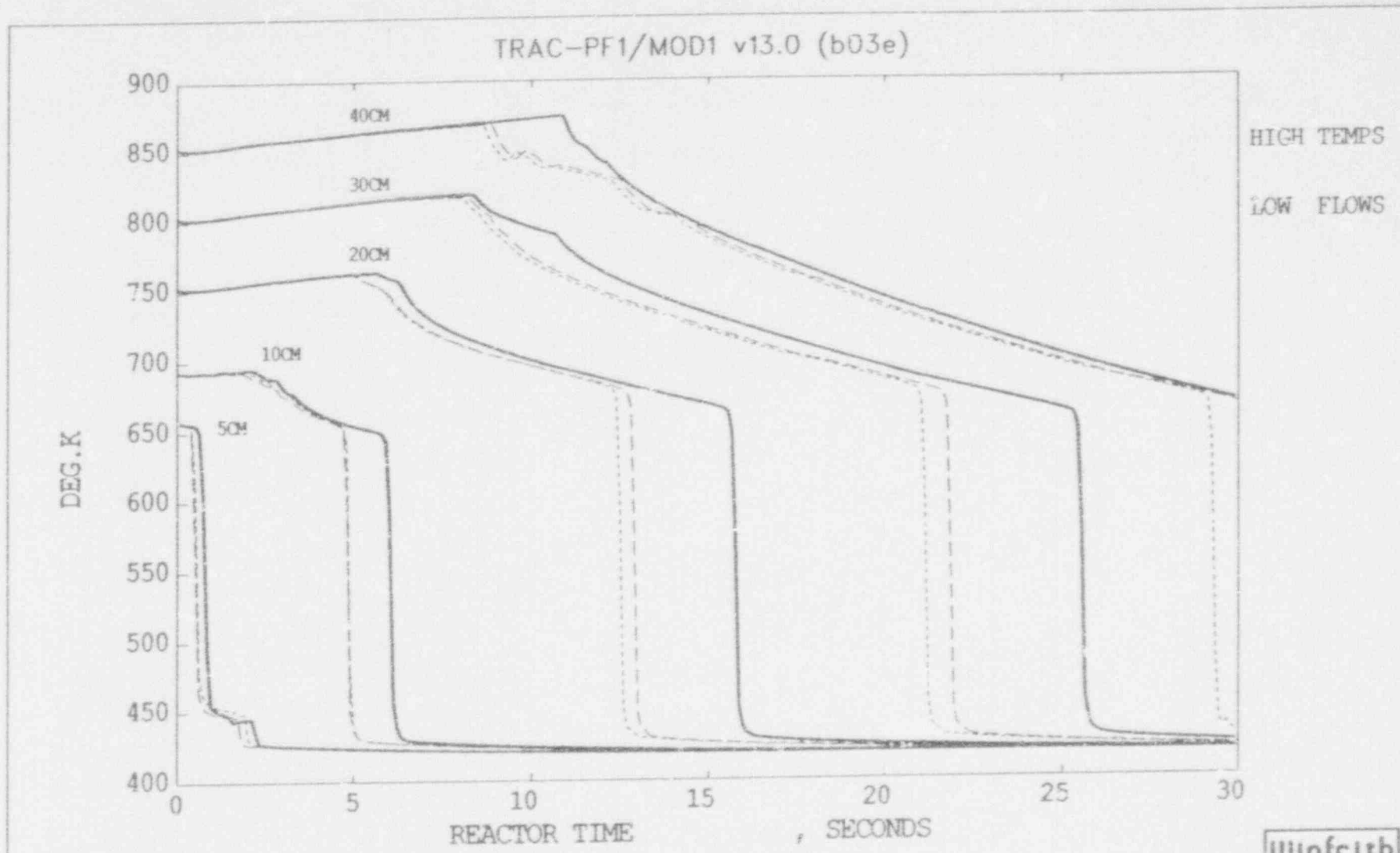


FIGURE 3

ROD SURFACE TEMPERATURES AT 5 ELEVATIONS, FOR 3 CALCULATIONS
 CALCULATIONS ARE: CONT=0.25MM, SHORT=0.05MM, LONG=0.25MM + 0.3MS DT

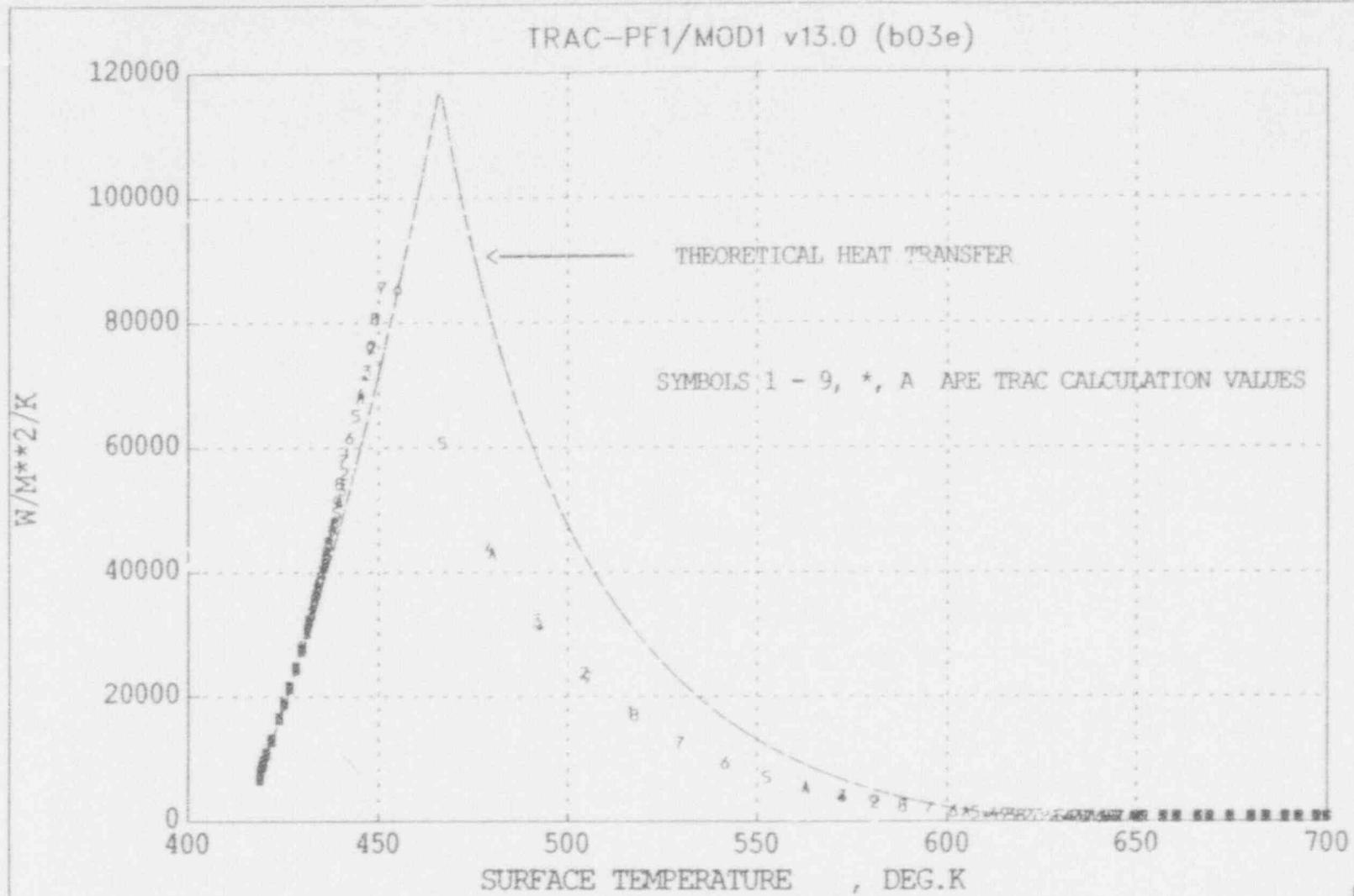
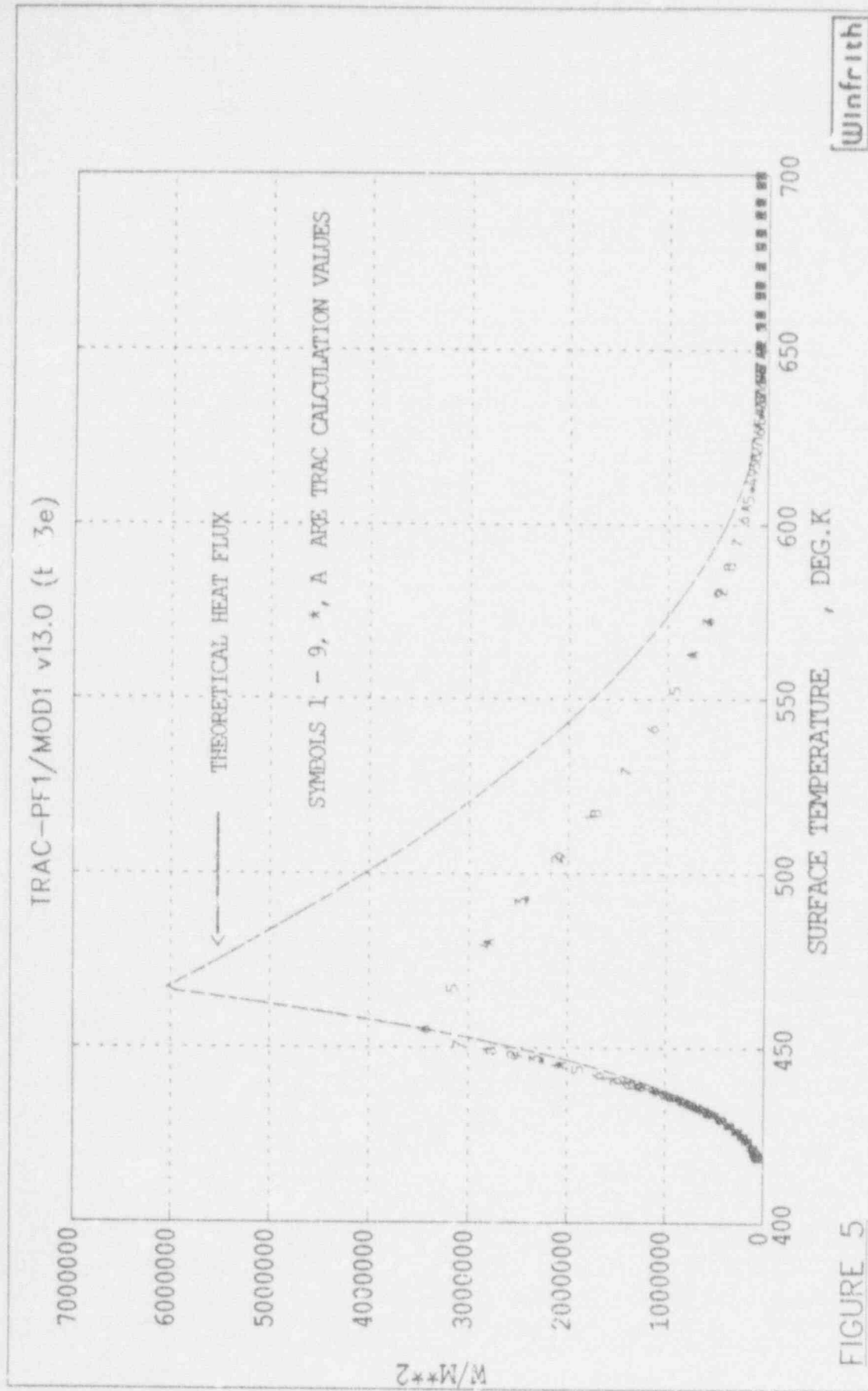


FIGURE 4

Winfrith

SURFACE-TO-FLUID HEAT TRANSFER COEFF. VS TEMPERATURE, AT 20 SECONDS
 TRAC CALCULATION WITH 0.25MM MIN MESH + THEORETICAL HEAT TRANSFER



[winfrith]

FIGURE 5

SURFACE-TO-FLUID HEAT FLUX VS TEMPERATURE, AT 20 SECONDS
 TRAC CALCULATION WITH 0.25MM MIN MESH + THEORETICAL HEAT FLUX

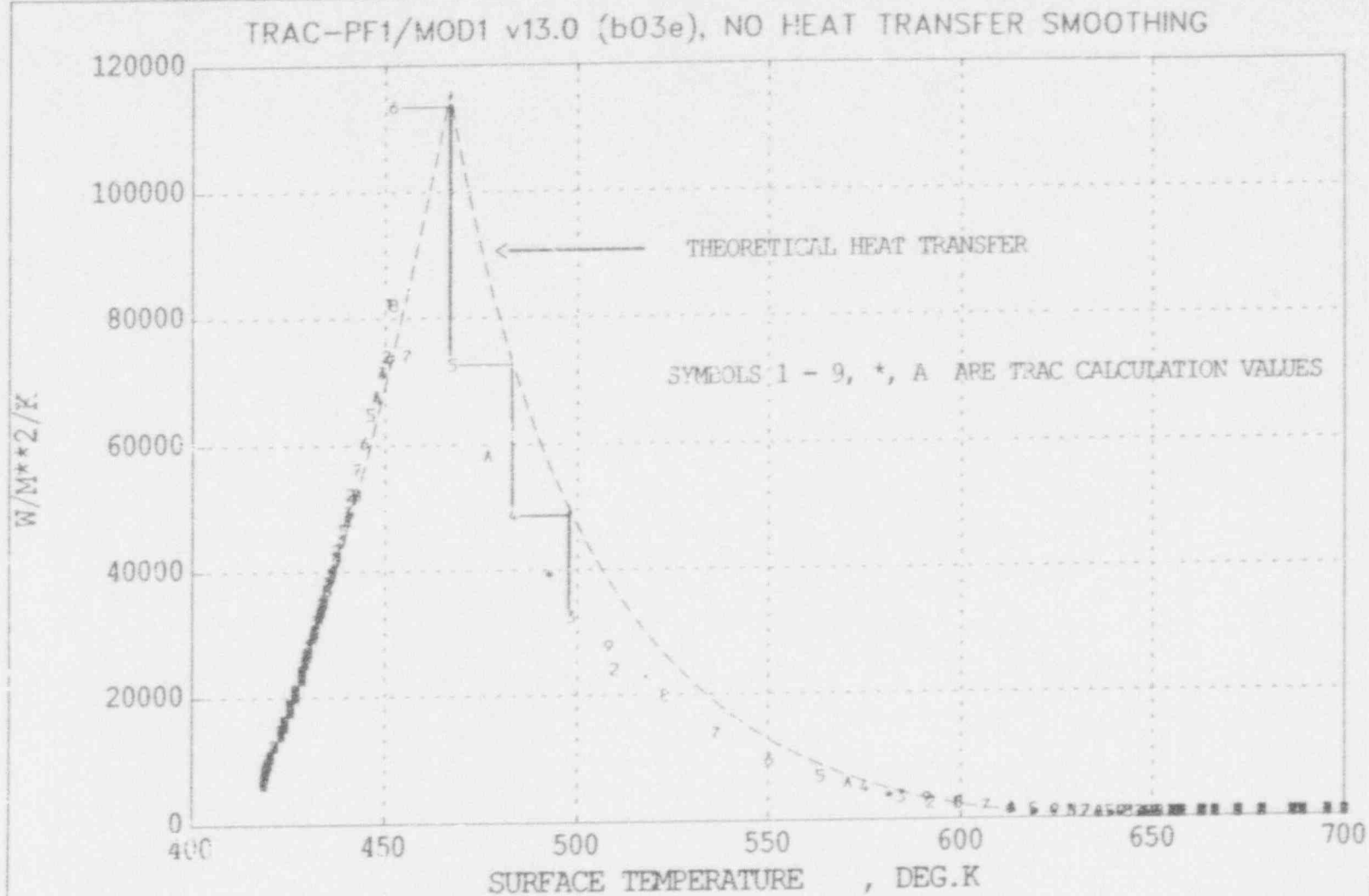


FIGURE 6

SURFACE-TO-FLUID HEAT TRANSFER COEFF. VS TEMPERATURE, AT 20 SECONDS
 TRAC CALC. WITH 0.25MM MIN MESH, NO SMOOTHING + THEORETICAL H. T.

Winfrith

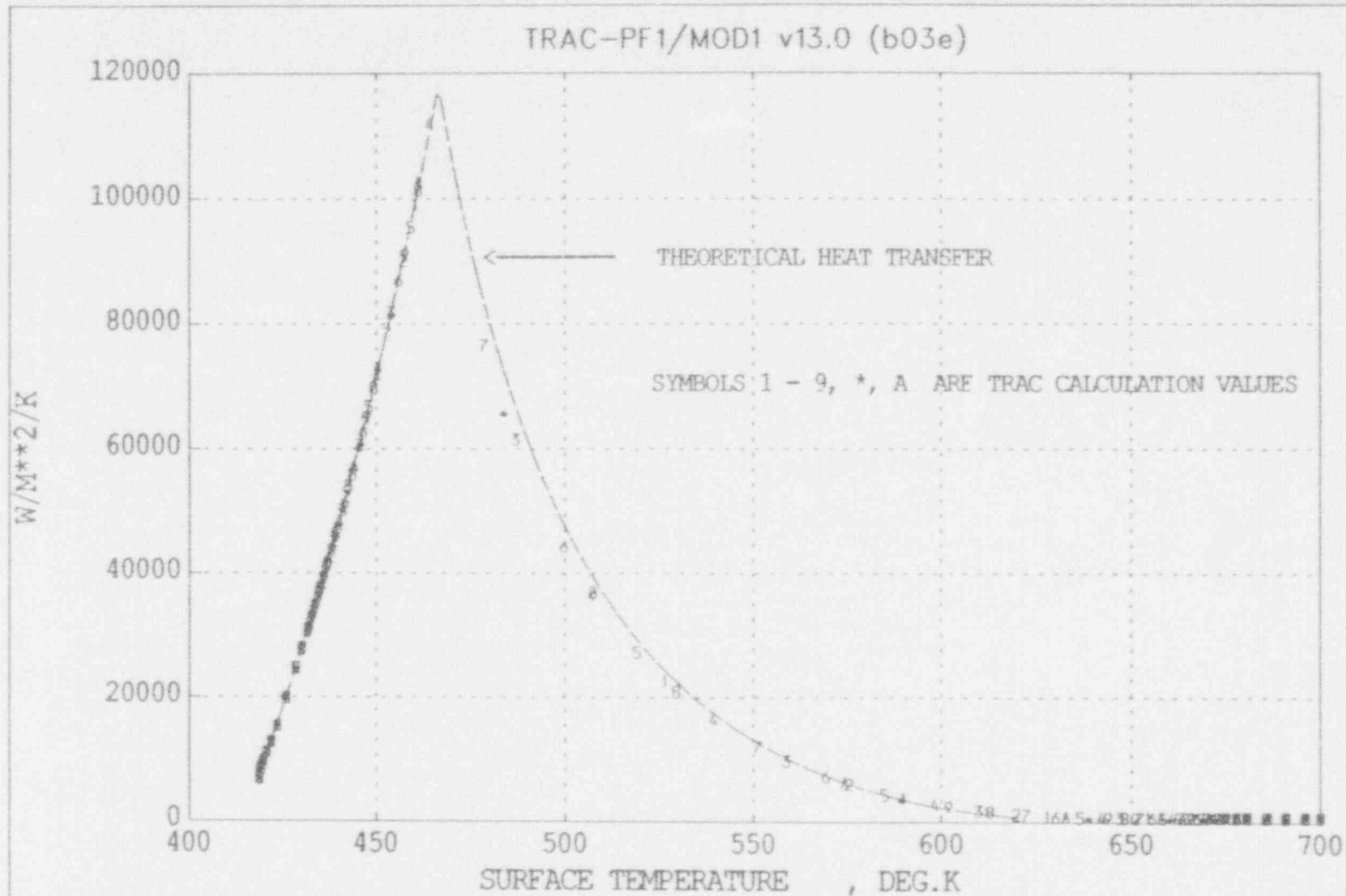
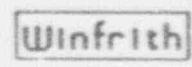


FIGURE 7



SURFACE-TO-FLUID HEAT TRANSFER COEFF. VS TEMPERATURE, AT 20 SECONDS
TRAC CALC. WITH 0.25MM MIN MESH, 0.3MS TIMESTEP + THEORETICAL H.T.

FIGURE 7

AEEW - M 2590

20

FWR/HTWG/P(89) 725

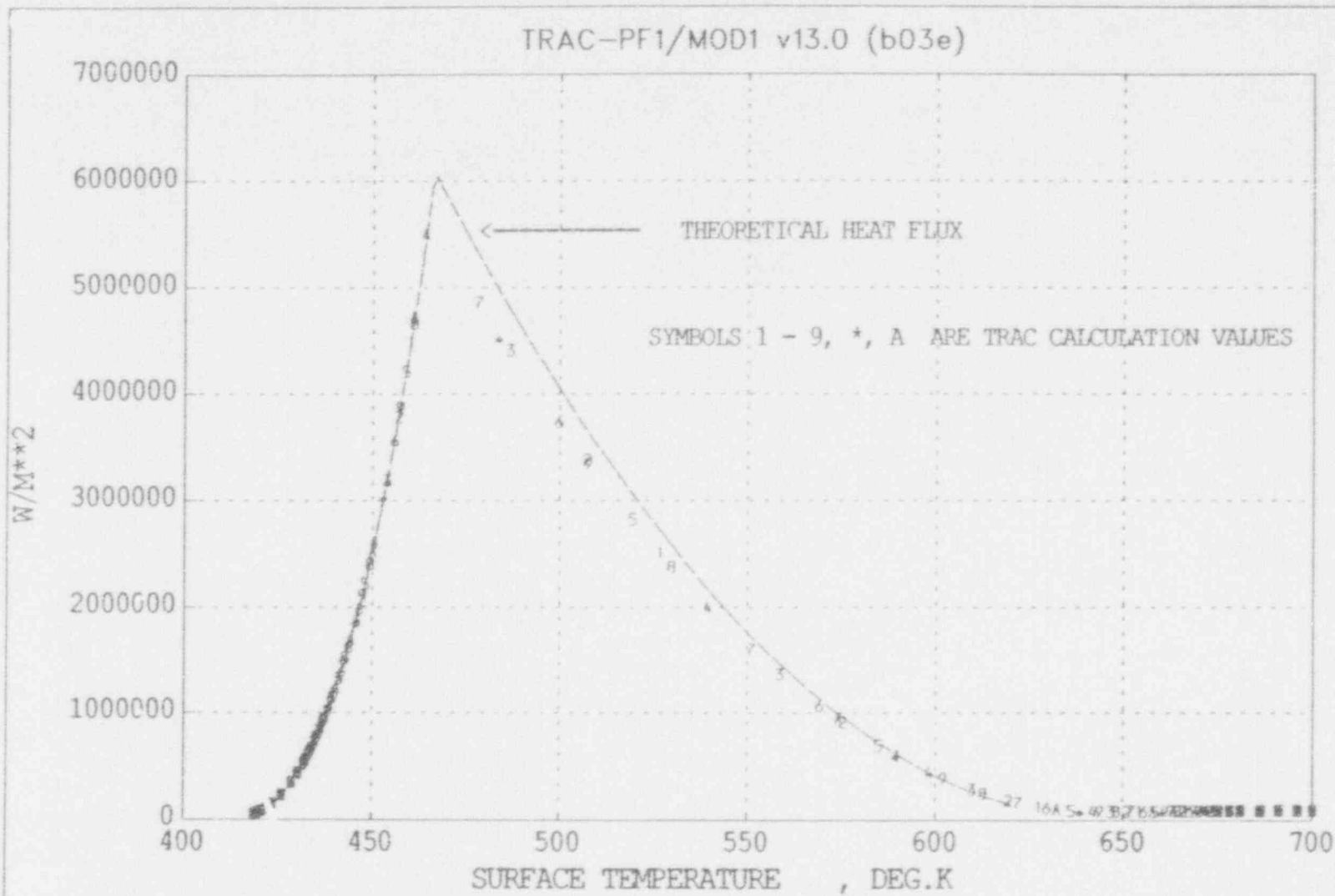


FIGURE 8

Winfrith

SURFACE-TO-FLUID HEAT FLUX VS TEMPERATURE, AT 20 SECONDS
TRAC CALC. WITH 0.25MM MIN MESH, 0.3MS TIMESTEP + THEORETICAL H.T.

FIGURE 8

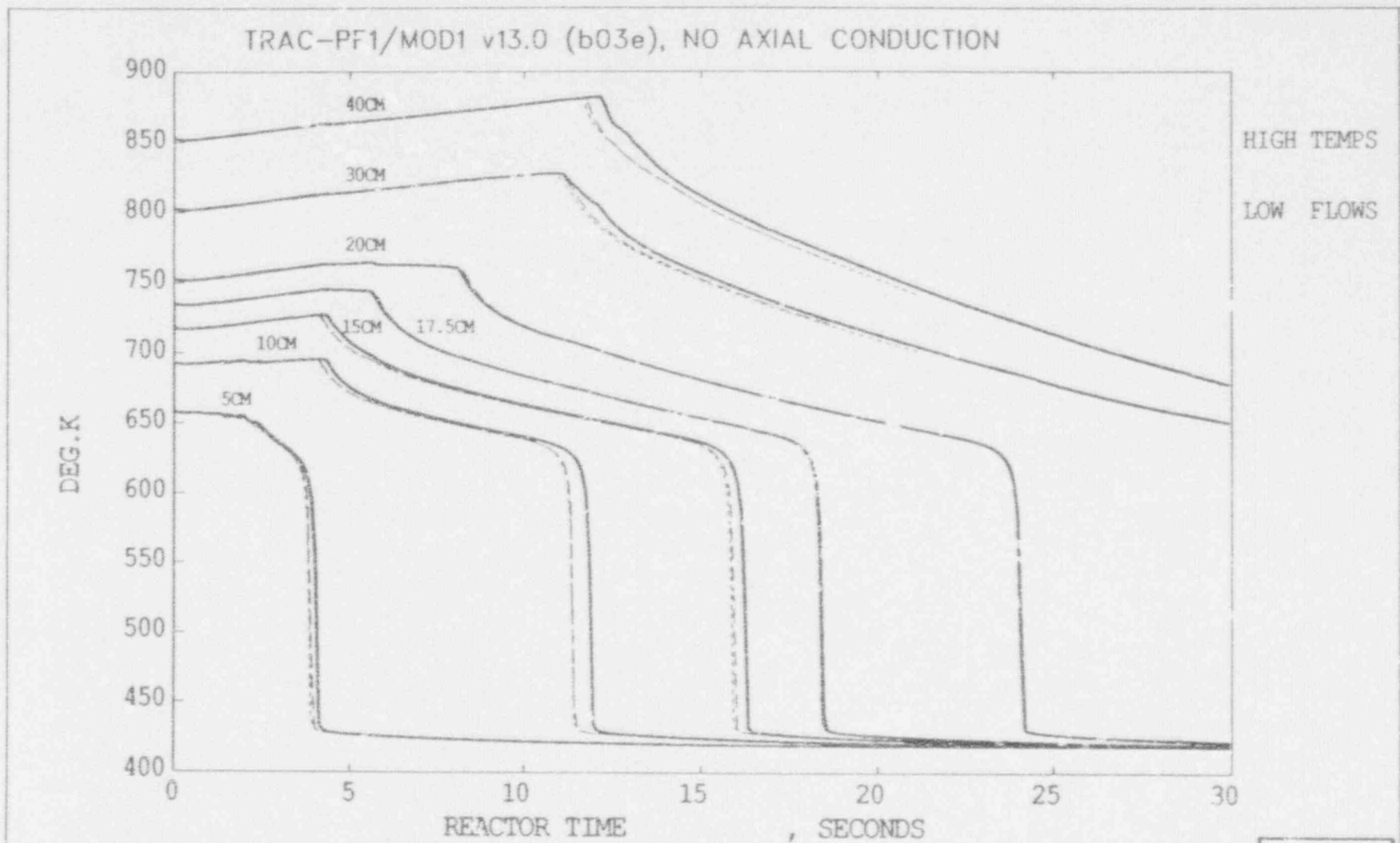


FIGURE 9

ROD SURFACE TEMPERATURES AT 7 ELEVATIONS, FOR 3 NO-AXIAL CALCS
CALCULATIONS ARE: CONT=0.25MM, SHORT=0.25MM+0.3MS, LONG=0.05MM+0.3MS

FIGURE 9

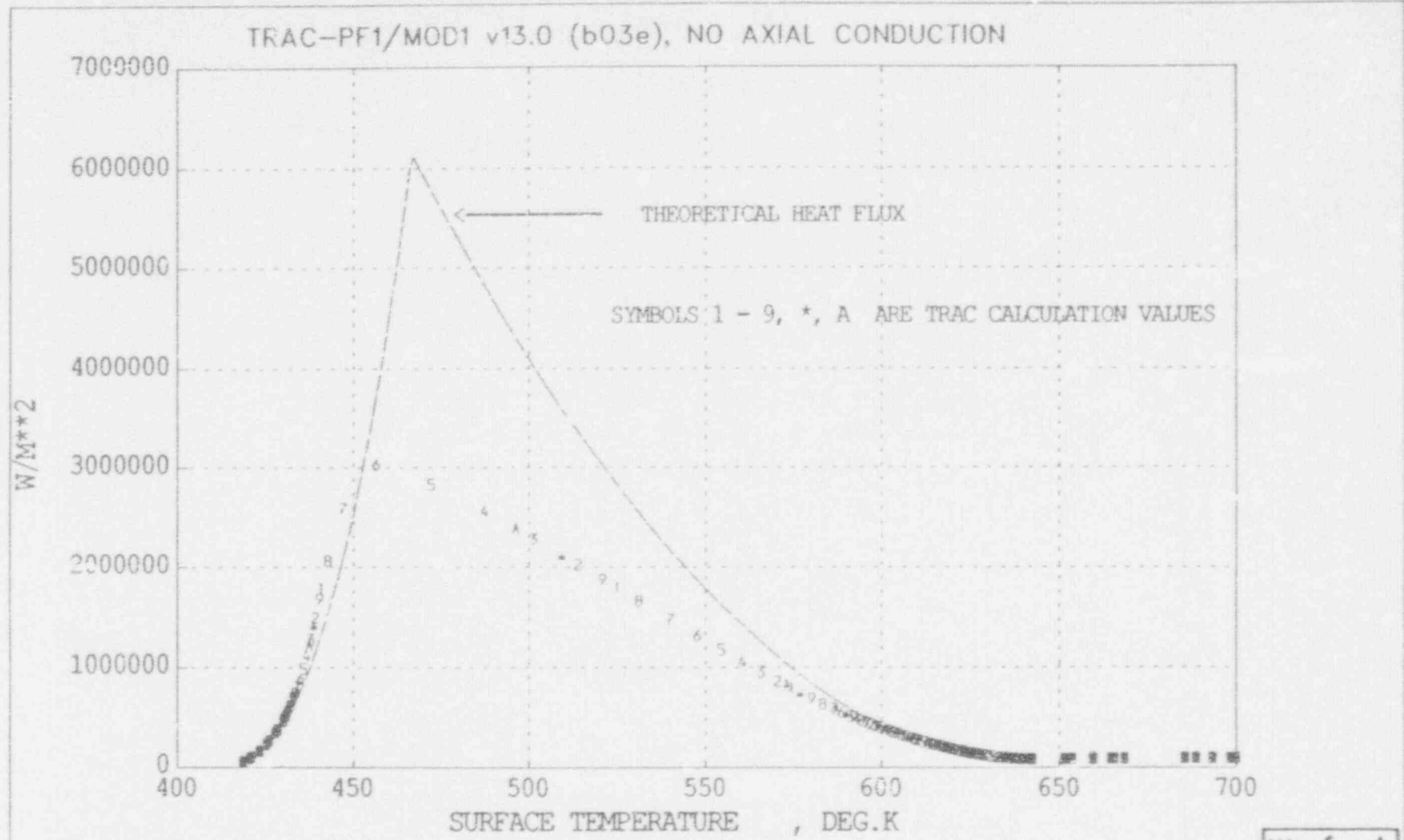
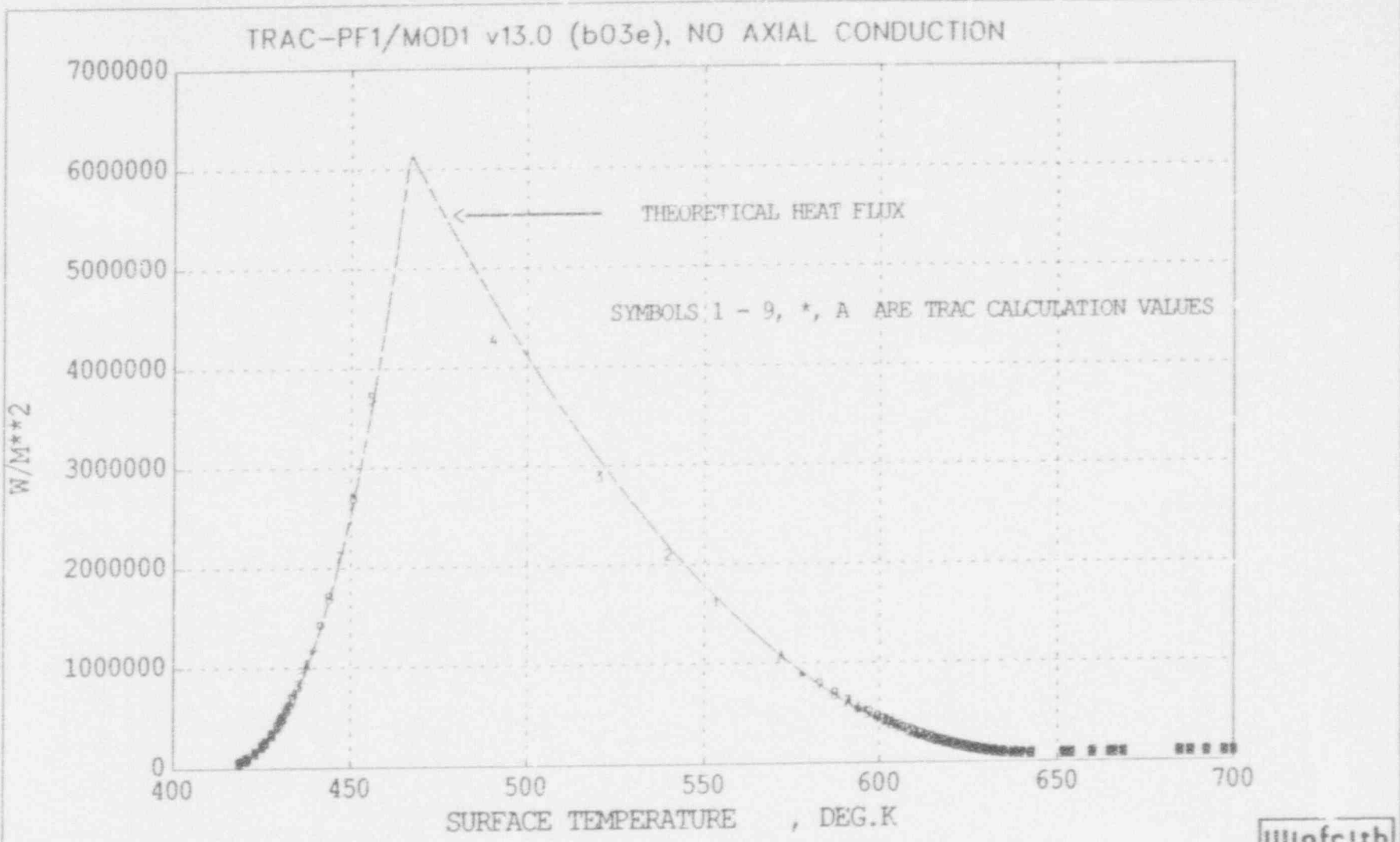


FIGURE 10

Winfrith

SURFACE-TO-FLUID HEAT FLUX VS TEMPERATURE, AT 20 SECS
 TRAC CALC, NO AXIAL CONDN, 0.25MM MIN MESH + THEORETICAL HEAT FLUX

FIGURE 10



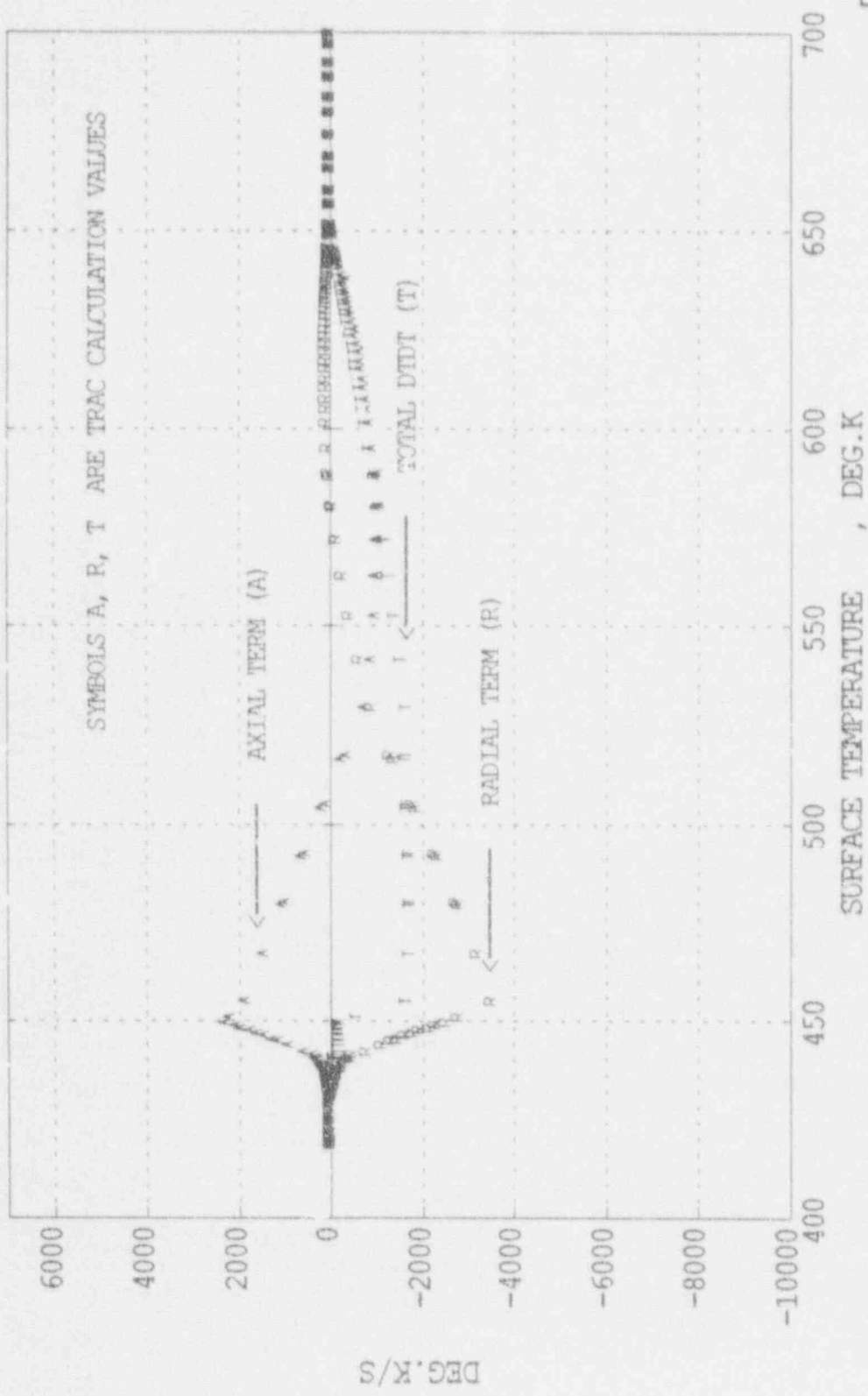
Winfrith

FIGURE 11

SURFACE-TO-FLUID HEAT FLUX VS TEMPERATURE, AT 20 SECONDS
 TRAC, NO AXIAL CONDN, 0.25MM MIN MESH, 0.3MS STEP + THEORETICAL H.T.

FIGURE 11

TRAC-PF1/MOD1 v13.0 (b03e)



Winfrith

FIGURE 12

HEAT CONDUCTION EQUATION: QUENCH FRONT PROFILE AT 20 SECONDS
TRAC CALCULATION WITH 0.25MM MIN MESH

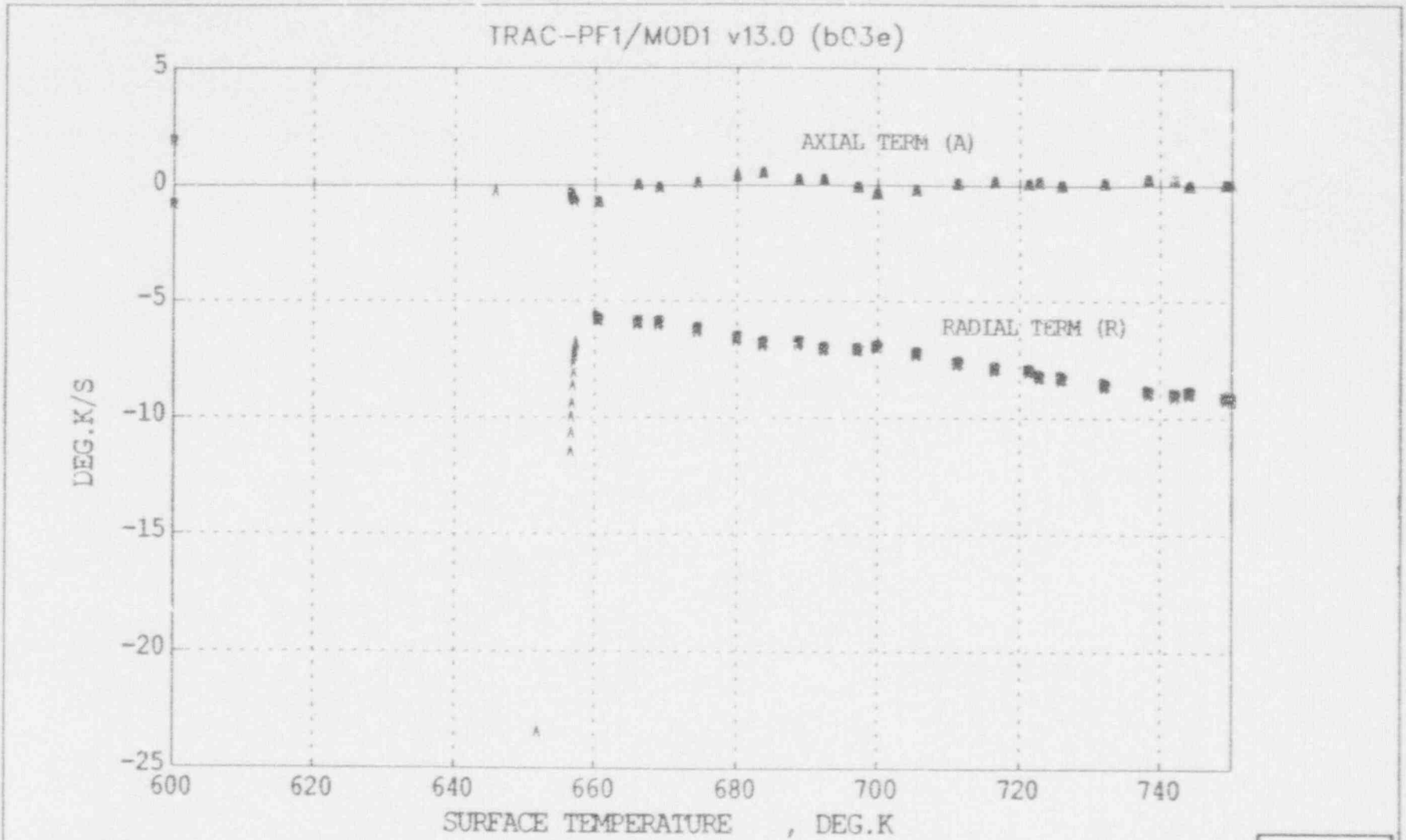


FIGURE 13

Winfrith

HEAT CONDUCTION EQUATION: QUENCH FRONT PROFILE AT 20 SECONDS
TRAC CALCULATION WITH 0.25MM MIN MESH [EXPLODED VIEW]

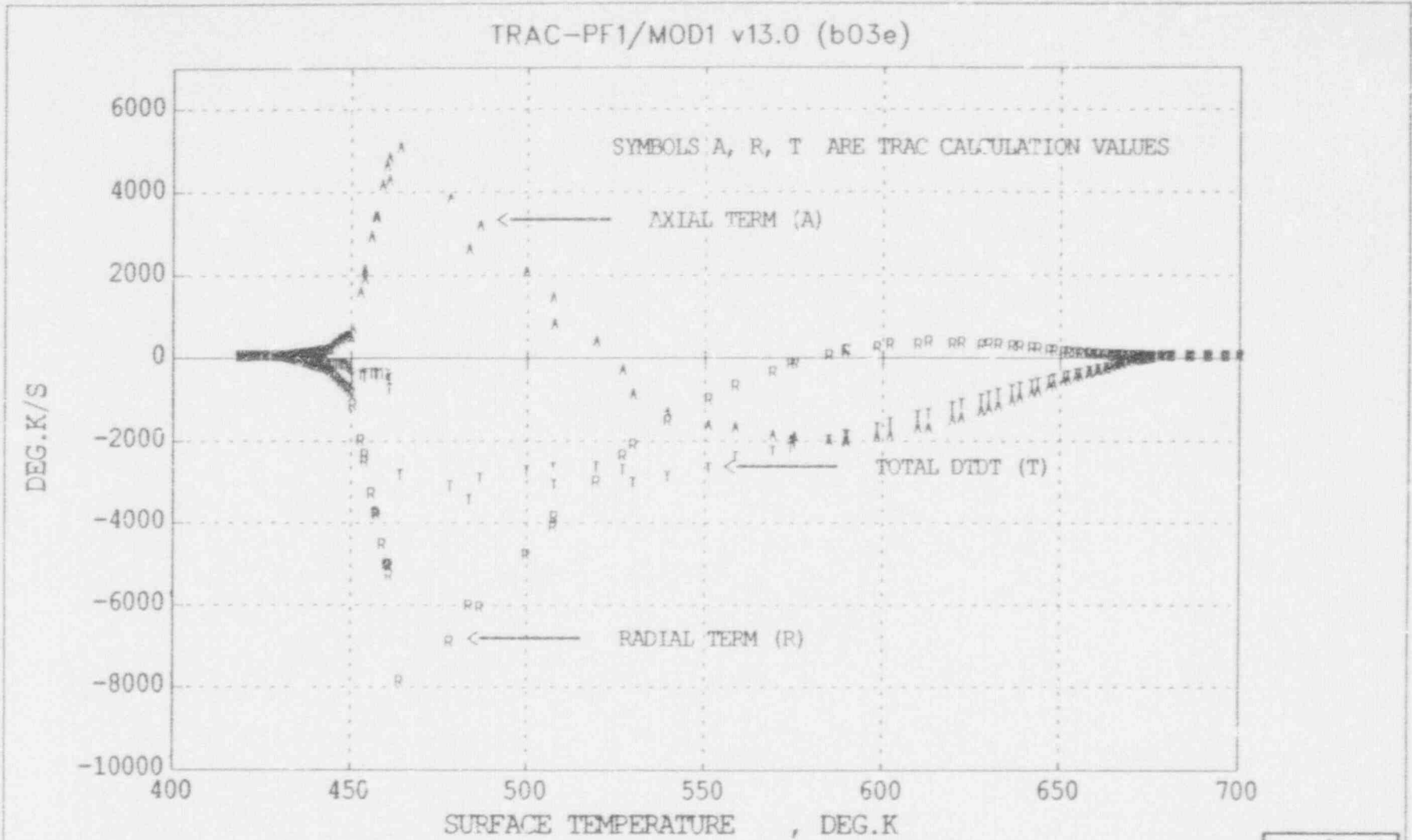


FIGURE 14

Winfrith

HEAT CONDUCTION EQUATION: QUENCH FRONT PROFILE AT 20 SECONDS
TRAC CALCULATION WITH 0.25MM MIN MESH, 0.3MS TIMESTEP

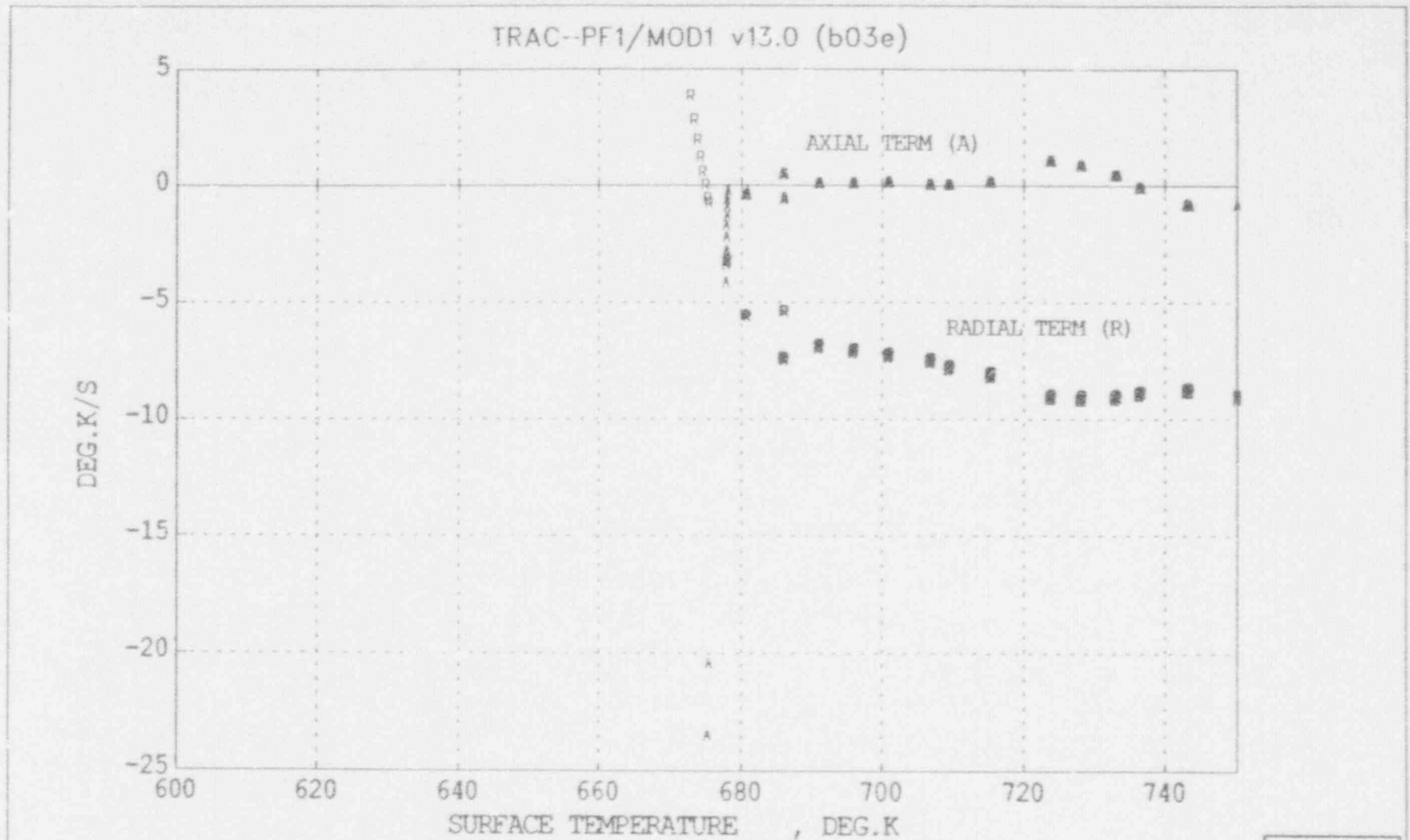


FIGURE 15

Winfrith

HEAT CONDUCTION EQUATION: QUENCH FRONT PROFILE AT 20 SECONDS
 TRAC CALCULATION WITH 0.25MM MIN MESH, 0.3MS TIMESTEP [EXPLODED VIEW]

AEEW - M 2590
28
PWR/HTWG/P(89) 725

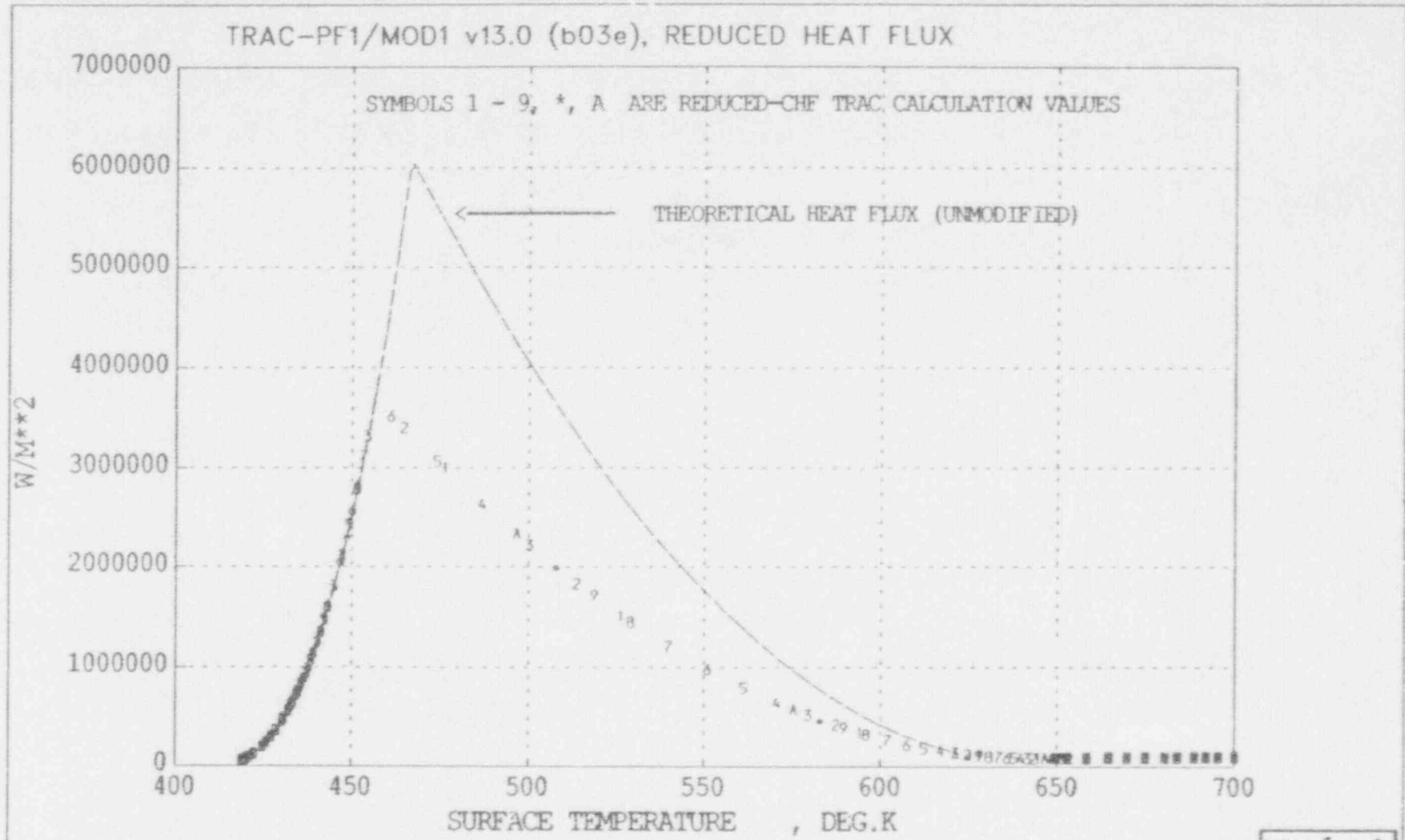
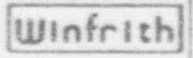


FIGURE 16



SURFACE-TO-FLUID HEAT FLUX VS TEMPERATURE, AT 20 SECONDS
TRAC CALC WITH 0.25MM MIN MESH, 0.3MS STEP, REDUCED CHF + THEORETICAL

FIGURE 16

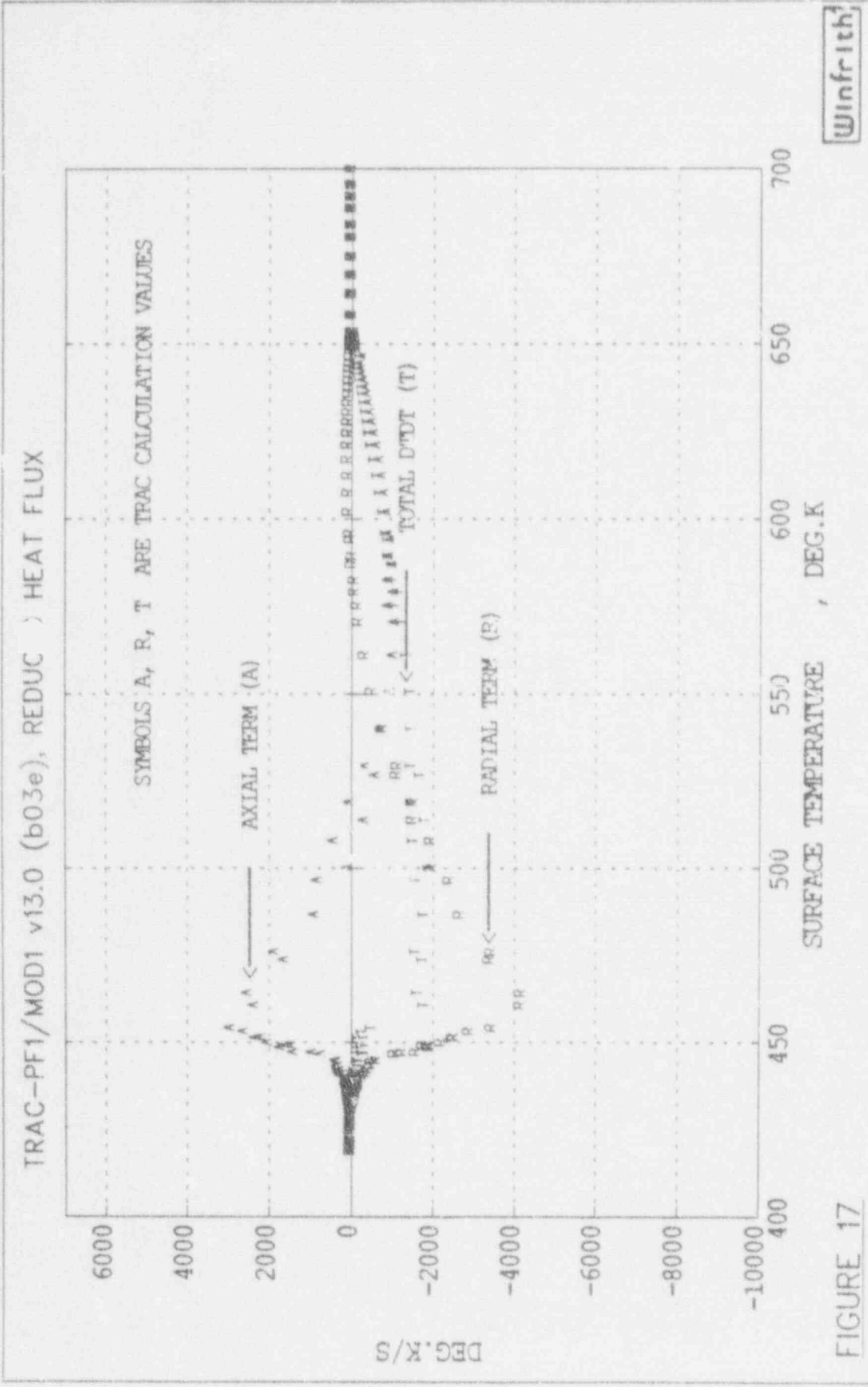


FIGURE 17

HEAT CONDUCTION EQUATION: QUENCH FRONT PROFILE AT 20 SECONDS
 TRAC CALCULATION WITH 0.25MM MIN MESH, 0.3MS STEP, REDUCED HEAT FLUX

AEEW - M 2590

30

PWR/HTWG/P(89) 725

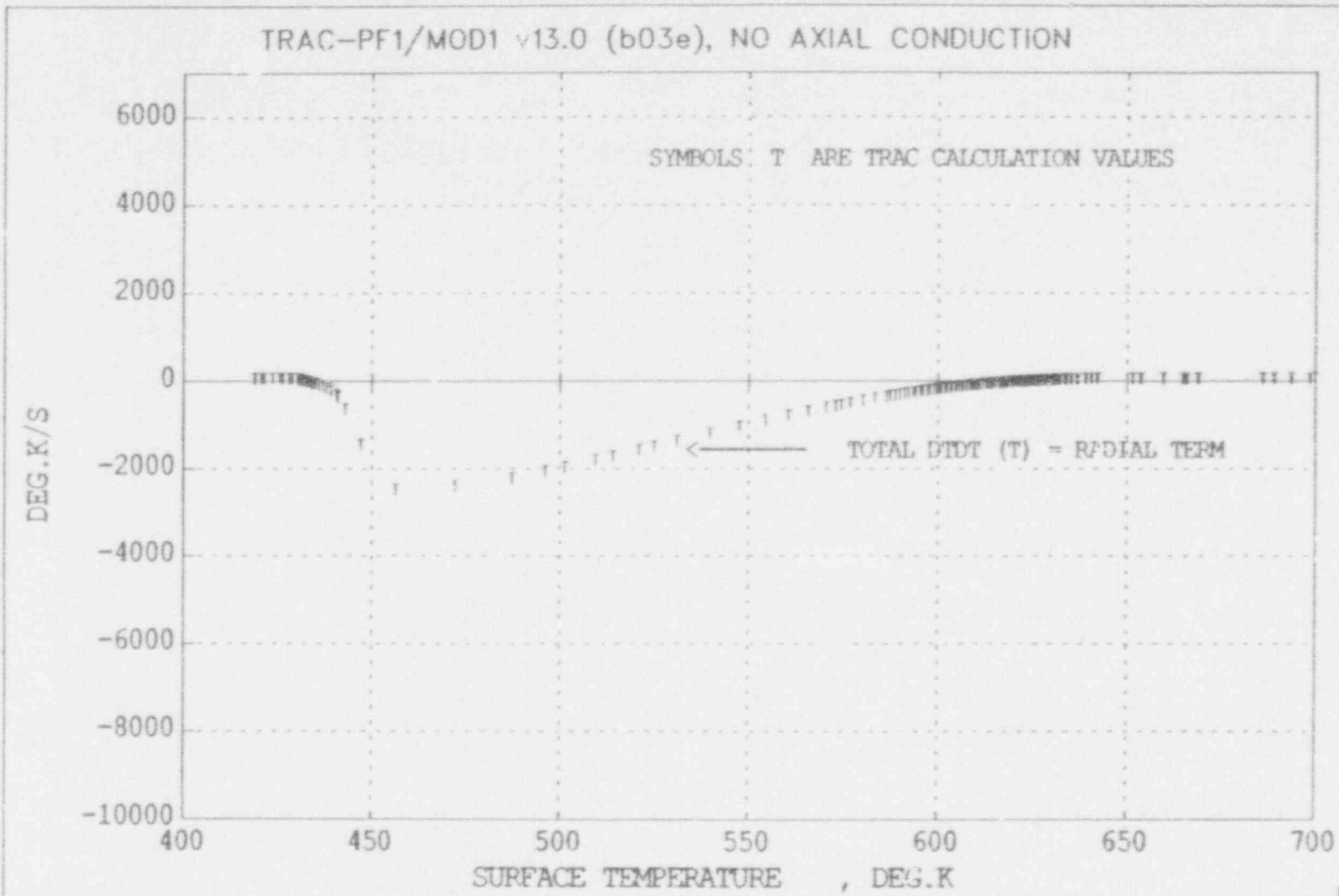


FIGURE 18

Winfrith

HEAT CONDUCTION EQUATION: QUENCH FRONT PROFILE AT 20 SECONDS
TRAC CALCULATION WITH NO AXIAL CONDN, 0.25MM MIN MESH

FIGURE 18

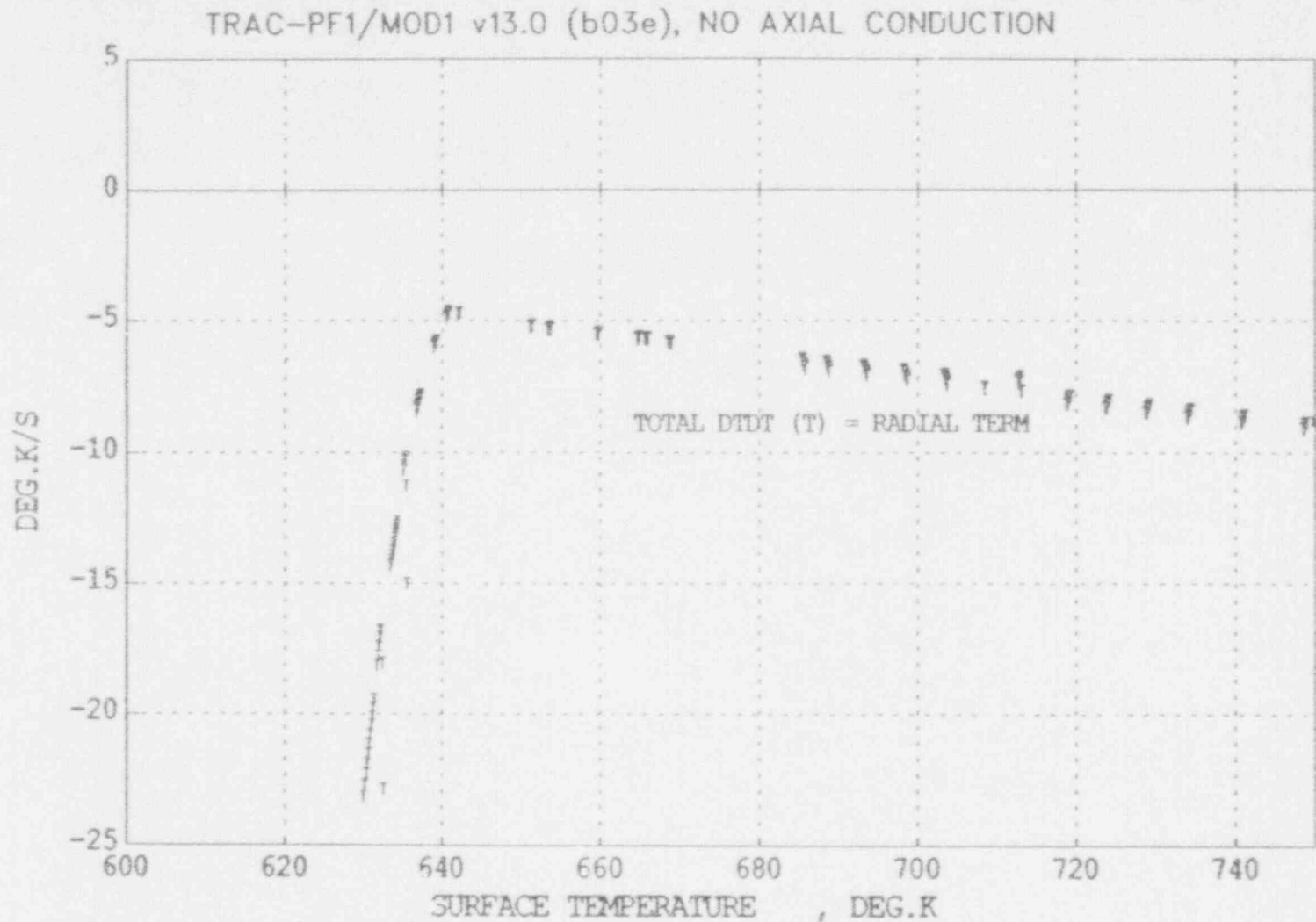


FIGURE 19

Winfrith

HEAT CONDUCTION EQUATION: QUENCH FRONT PROFILE AT 20 SECONDS
TRAC CALC WITH NO AXIAL CONDN, 0.25MM MIN MESH [EXPLoded VIEW]

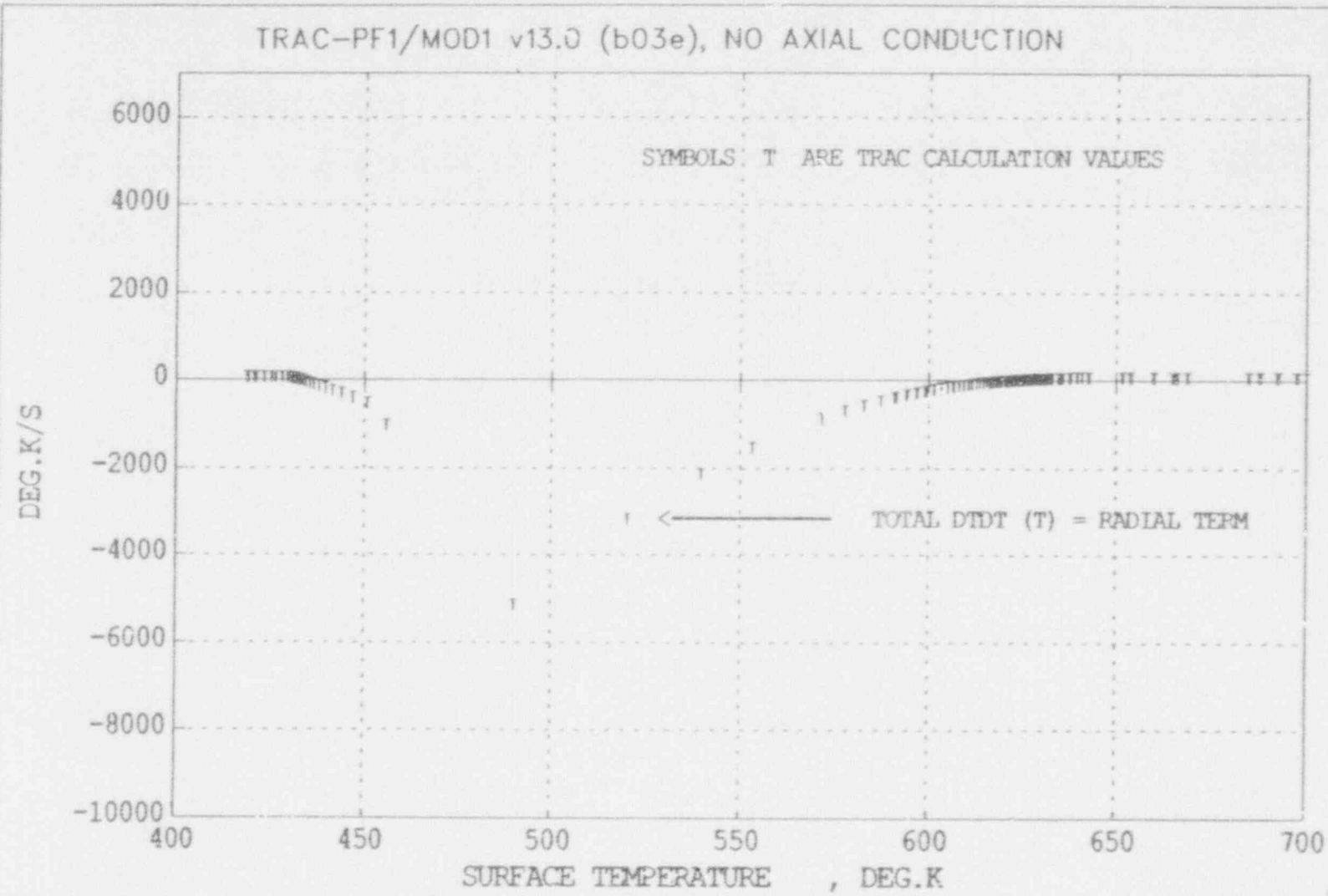
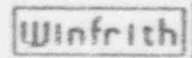


FIGURE 20



HEAT CONDUCTION EQUATION: QUENCH FRONT PROFILE AT 20 SECONDS
TRAC CALC WITH NO AXIAL CONDN, 0.25MM MIN MESH, 0.3MS TIMESTEP

FIGURE 20

AEEW - M 2590

33

PWR/HTWG/P(89) 725

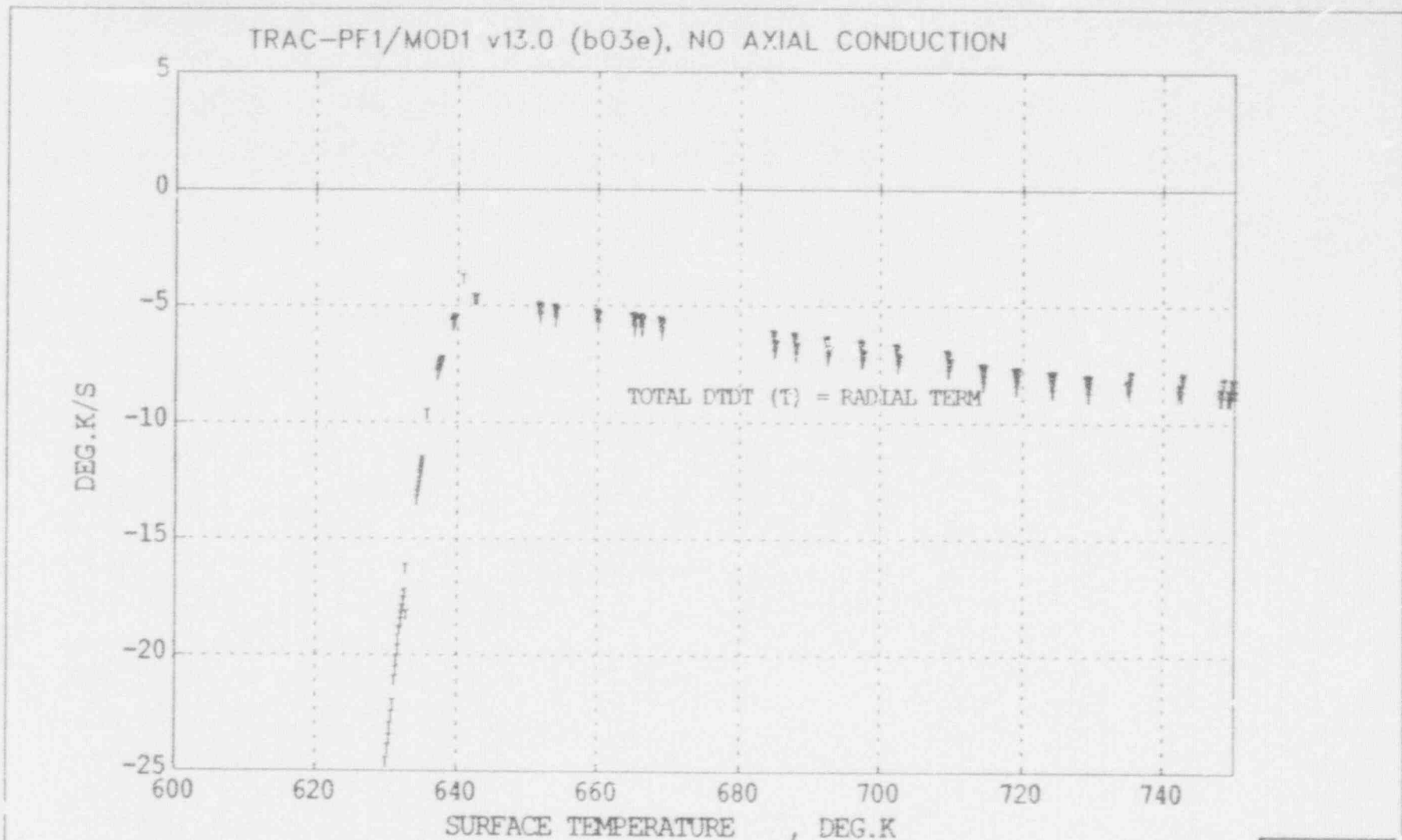


FIGURE 21

Winfrith

HEAT CONDUCTION EQUATION: QUENCH FRONT PROFILE AT 20 SECONDS
TRAC WITH NO AXIAL COND, 0.25MM MIN MESH, 0.3MS STEP [EXPLODED VIEW]

FIGURE 21

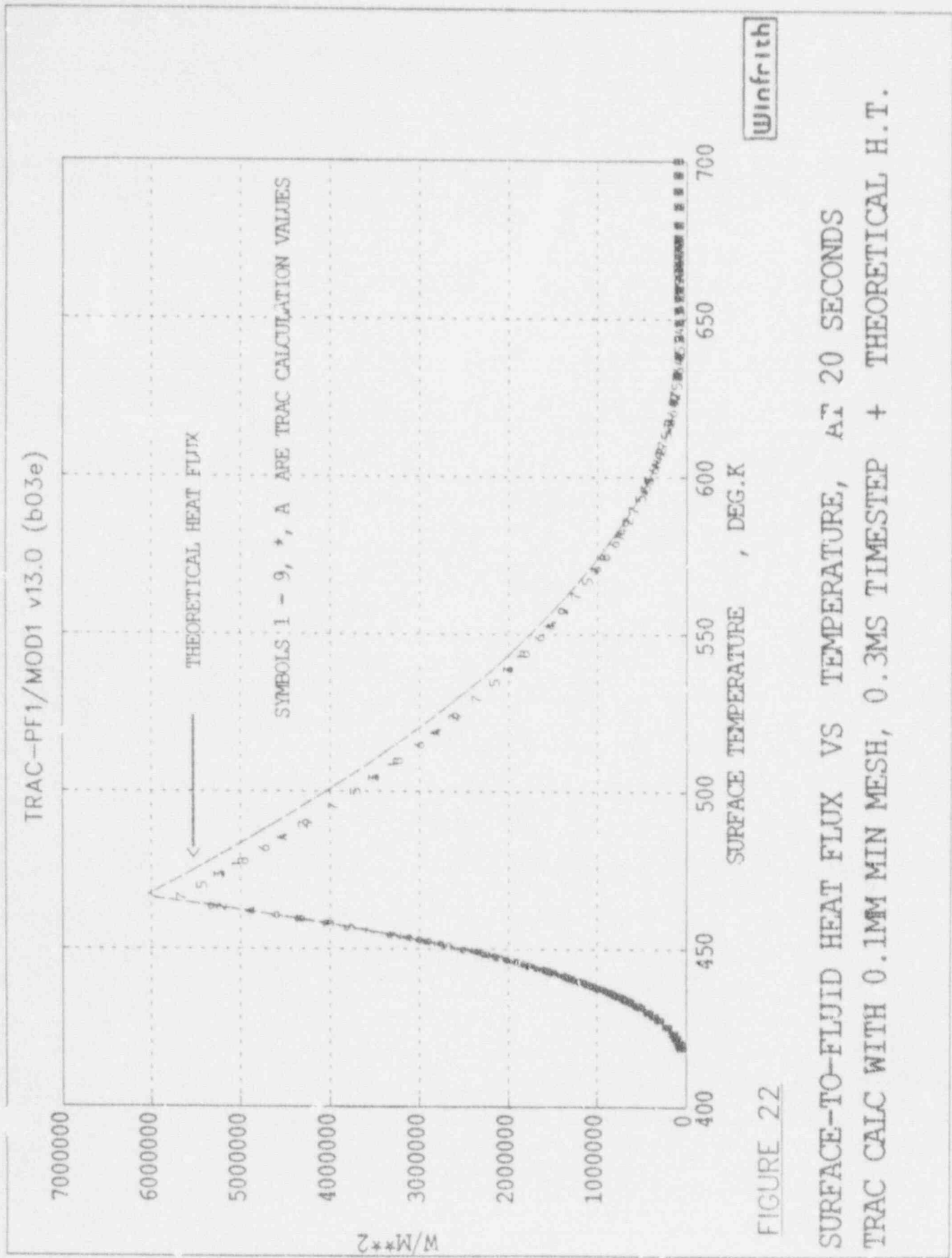


FIGURE 22

SURFACE-TO-FLUID HEAT FLUX VS TEMPERATURE, AT 20 SECONDS
 TRAC CALC WITH 0.1MM MIN MESH, 0.3MS TIMESTEP + THEORETICAL H.T.

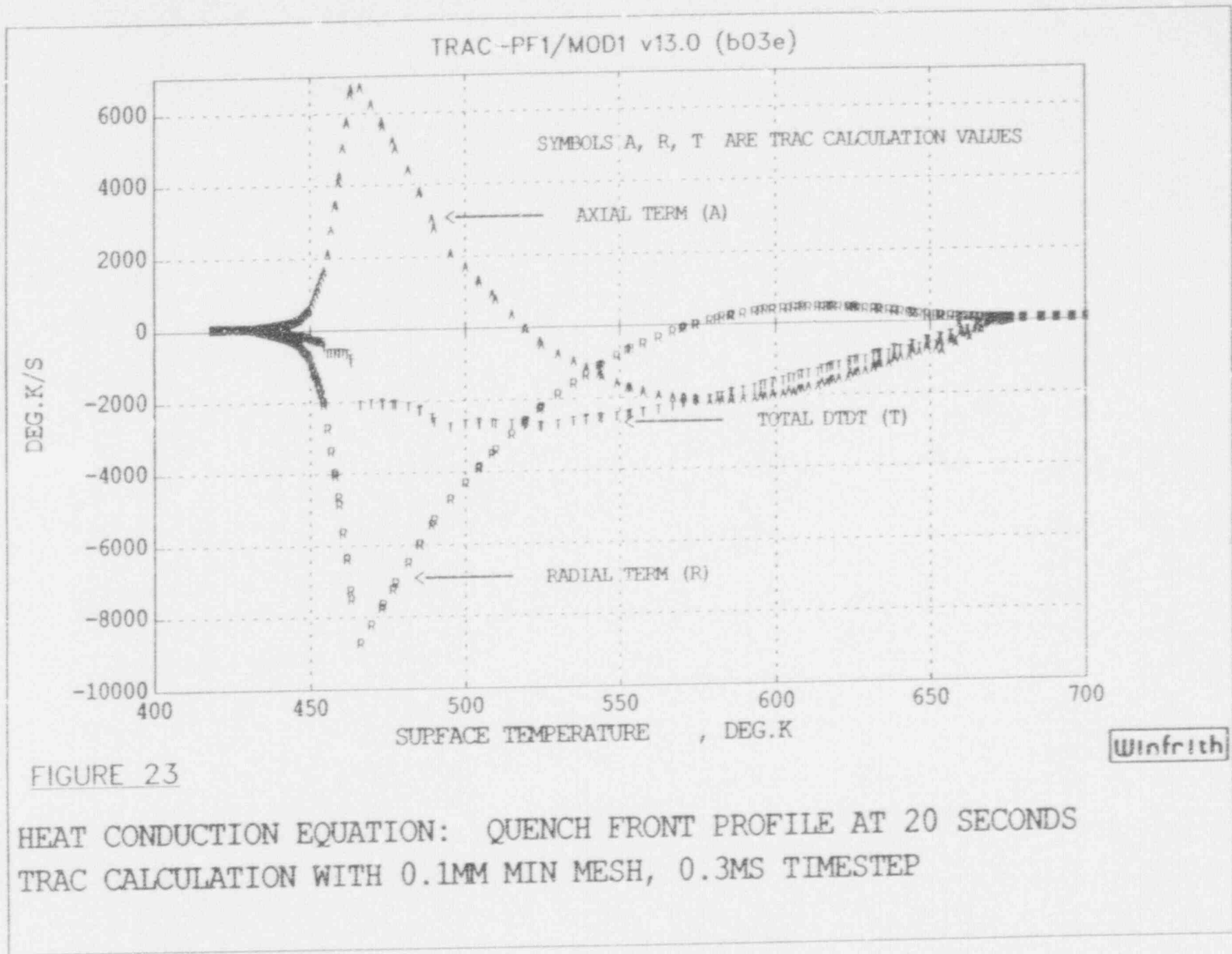


FIGURE 23

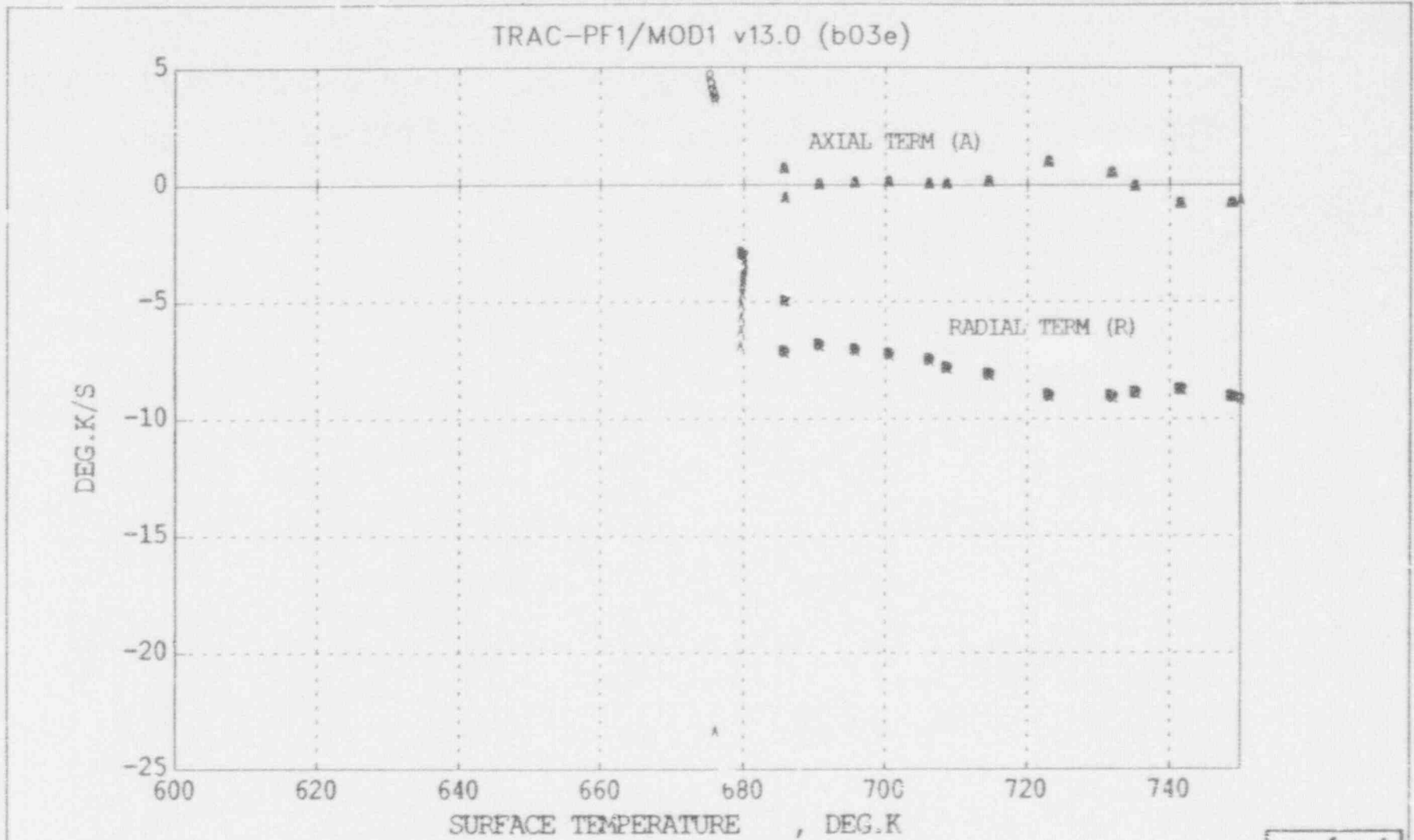


FIGURE 24

Winfrith

HEAT CONDUCTION EQUATION: QUENCH FRONT PROFILE AT 20 SECONDS
 TRAC CALC WITH 0.1MM MIN MESH, 0.3MS TIMESTEP [EXPLODED VIEW]

FIGURE 24

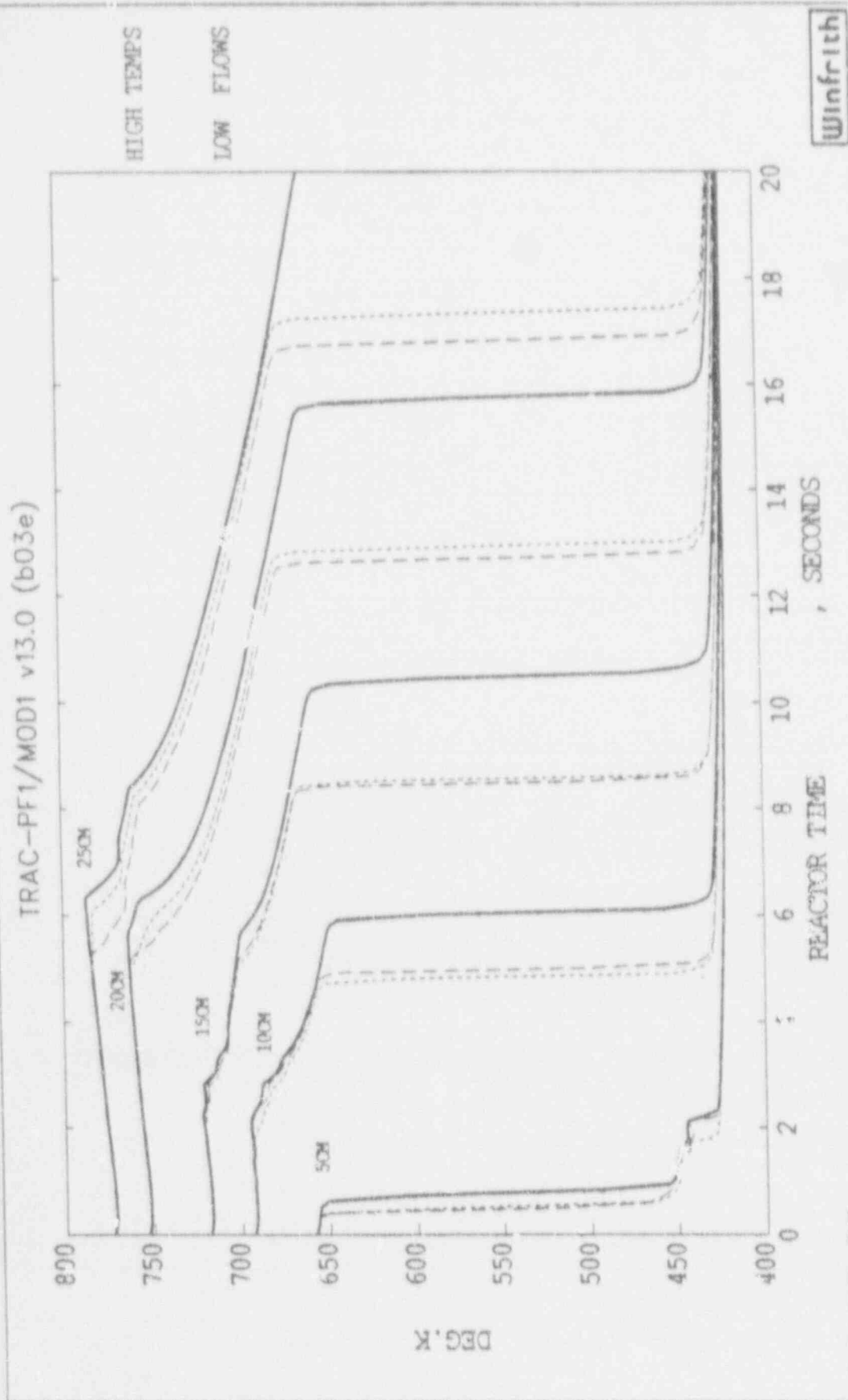


FIGURE 25

ROD SURFACE TEMPERATURES AT 5 ELEVATIONS, FOR 3 CALCULATIONS
 CALCS ARE: CONT=0.25MM, SHORT=0.25MM + 0.3MS DT, LONG=0.1MM + 0.3MS DT

FIGURE 25

DISTRIBUTION

PWR HEAT TRANSFER AND HYDRAULICS WORKING GROUP

Mr M W E Coney	CEGB	TEC Leatherhead
Dr C A Cooper	WTC	342/B41
Dr G R Kimber	WTC	233/A32
Mr I Brittain	WTC	201/A32
Mr K G Pearson	WTC	338/B41
Dr D B Utton	NNC	Booths Hall, Chelford Road, Knutsford, Cheshire WA16 9QZ
Dr P A W Bratby	NNC	Booths Hall, Chelford Road, Knutsford, Cheshire
Mr D Coucill	BNF	Springfields Works, Salwick, Preston, Lancs
Mr P C Hall	CEGB	TD, Barnett Way, Barnwood, Gloucestershire
Dr P R Farmer	CEGB	National Power, Room C1016, Courtenay House, 18 Warwick Lane London EC4P 3EB
Dr L Daniels	UKAEA	Bldg 392, AERE Harwell
Mr D K Tong	UKAEA	CLF 125, SRD Culcheth, Warrington
Mr B Chojnowski	CEGB	Marchwood Engineering Labs, Marchwood, Southampton
Dr M El-Shanawany	CEGB	National Power, Nuclear Safety Branch Courtenay House, 18 Warwick Lane, London EC4P 3EB
Mr K Meador	CEGB	PPG, Booths Hall, Chelford Road, Knutsford, Cheshire
Mr P L Catfoot	CEGB	PPG, Booths Hall, Chelford Road, Knutsford, Cheshire

WTC, DORCHESTER, DORSET, DT2 8DH

Dr I H Gibson	236/A32	(Summary Only)
Dr C Richards	260/A32	
Dr A T D Butland	343/B41	
Dr M K Denham	336/B41	
Dr A J Wickett	266/A32	
Mr R O'Mahoney	263/A32	(10 copies)
Dr W M Bryce	262/A32	
Dr B J Holmes	264/A32	
Mr G Ward	239/A32	
Mr P I R Jones	231/A32	

NUCLEAR INSTALLATIONS INSPECTORATE, HEALTH AND SAFETY EXECUTIVE, ST PETERS
HOUSE, STANLEY PRECINCT, BALLIOL ROAD, BOOTLE, L20 3LZ

Mr C Potter
Mr J F Campbell (Summary Only)
Dr S A Harbison (Summary Only)

INTERNATIONAL CODE ASSESSMENT AND APPLICATIONS PROGRAMME

USNRC, 5650 NICHOLSON LANE, ROCKVILLE, MARYLAND 20814, USA

Mr G Rhee (2 copies)
Mr D Bessette

EG&G (IDAHO) INC, INEL, PO BOX 1625, IDAHO FALLS, IDAHO 83415, USA

Mr R Shultz (2 copies + single sided copy)
Mr R Hanson
Dr G Wilson

LOS ALAMOS NATIONAL LABORATORY, PO BOX 1663, LOS ALAMOS, NEW MEXICO 87545, USA

Mr N Schnurr (2 copies)
Dr R A Nelson
Dr M Capiello
Mr R Jenks

PAUL SCHERRER INSTITUTE, CH-5303, WÜRENLINGEN, SWITZERLAND

Dr S N Aksan
Dr P Coddington

JAERI, TOKAI-MURA, NAKA-GUN, IBARAKI-KEN, 31911, JAPAN

Dr Y Murao
Dr H Akimoto

DERS, CEA, BP NO 6, F-92260, FONTENAY-AUX-ROSES, FRANCE

Dr R Pochard

LIBRARIES

Dounreay	-2
Harwell	-2
Risley	-4
Windscale	-2
Winfrith	-4

BIBLIOGRAPHIC DATA SHEET

(See instructions on the reverse.)

REPORT NUMBER
(Assigned by NRC. Add Vol., Supp., Rev.,
and Addendum Numbers, if any.)

NUREG/IA-0073
AEEW-M2590

2. TITLE AND SUBTITLE

Time Step and Mesh Size Dependencies in the Heat Conduction
Solution of a Semi-Implicit, Finite Difference Scheme for
Transient Two-Phase Flow

3. DATE REPORT PUBLISHED

MONTH YEAR

April 1992

4. FIN OR GRANT NUMBER

A4682

5. AUTHOR(S)

R. O'Mahoney

6. TYPE OF REPORT

Technical

7. PERIOD COVERED (Include Dates)

8. PERFORMING ORGANIZATION - NAME AND ADDRESS (If NRC, provide Division, Office or Region, U.S. Nuclear Regulatory Commission, and mailing address. If contractor, provide name and mailing address.)

Winfrith Technology Centre
United Kingdom Atomic Energy Authority
Dorchester, Dorset, DT2 8DH
United Kingdom

9. SPONSORING ORGANIZATION - NAME AND ADDRESS (If NRC, type "Same as above". If contractor, provide NRC Division, Office or Region, U.S. Nuclear Regulatory Commission, and mailing address.)

Office of Nuclear Regulatory Research
U.S. Nuclear Regulatory Commission
Washington, DC 20555

10. SUPPLEMENTARY NOTES

11. ABSTRACT (200 words or less)

This report examines, and establishes the causes of, previously identified time step and mesh size dependencies. These dependencies were observed in the solution of a coupled system of heat conduction and fluid flow equations as used in the TRAC-PF1/MOD1 computer code. The report shows that a significant time step size dependency can arise in calculations of the quenching of a previously unwetted surface. The cause of this dependency is shown to be the explicit evaluation, and subsequent smoothing, of the term which couples the heat transfer and fluid flow equations. An axial mesh size dependency is also identified, but this is very much smaller than the time step size dependency. The report concludes that the time step size dependency represents a potential limitation on the use of large time step sizes for the types of calculation discussed. This limitation affects the present TRAC-PF1/MOD1 computer code and may similarly affect other semi-implicit finite difference codes that employ similar techniques. It is likely to be of greatest significance in codes where multi-step techniques are used to allow the use of large time steps.

12. KEY WORDS/DESCRIPTORS (List words or phrases that will assist researchers in locating the report.)

Time Step, Mesh Size, Dependencies, Heat Conduction Solution,
Transient Two-Phase Flow

13. AVAILABILITY STATEMENT

Unlimited

14. SECURITY CLASSIFICATION

(This Page)

Unclassified

(This Report)

Unclassified

15. NUMBER OF PAGES

16. PRICE

THIS DOCUMENT WAS PRINTED USING RECYCLED PAPER

NUREG/IA-0073

TIME STEP AND MESH SIZE DEPENDENCIES IN THE HEAT CONDUCTION SOLUTION OF
A SEMI-IMPLICIT, FINITE DIFFERENCE SCHEME FOR TRANSIENT TWO-PHASE FLOW

APRIL 1992

UNITED STATES
NUCLEAR REGULATORY COMMISSION
WASHINGTON, D.C. 20555

FIRST CLASS MAIL
POSTAGE AND FEES PAID
USNRC
PERMIT NO. G-87

OFFICIAL BUSINESS
PENALTY FOR PRIVATE USE, \$300

120555139531 1 14N1CI
US NRC-0ADM
DIV FOIA & PUBLICATIONS SVCS
IPS-PDR-NUREG
P-211
WASHINGTON DC 20555